

Differentially Private Federated Low Rank Adaptation Beyond Fixed-Matrix

Ming Wen*

Department of Electronic Engineering
Fudan University
mwenz3@m.fudan.edu.cn

Jiaqi Zhu†

Department of Electronic Engineering
Fudan University
21307130391@m.fudan.edu.cn

Yuedong Xu

Department of Electronic Engineering
Fudan University
ydxu@fudan.edu.cn

Yipeng Zhou

School of Computing
Macquarie University
yipeng.zhou@mq.edu.au

Dingding Han

Department of Communication Science and Engineering
Fudan University
ddhan@fudan.edu.cn

Abstract

Large language models (LLMs) typically require fine-tuning for domain-specific tasks, and LoRA offers a computationally efficient approach by training low-rank adapters. LoRA is also communication-efficient for federated LLMs when multiple users collaboratively fine-tune a global LLM model without sharing their proprietary raw data. However, even the transmission of local adapters between a server and clients risks serious privacy leakage. Applying differential privacy (DP) to federated LoRA encounters a dilemma: adding noise to both adapters amplifies synthetic noise on the model, while fixing one adapter impairs the learnability of fine-tuning. In this paper, we propose FedASK (Differentially Private **F**ederated Low Rank Adaptation with Double **S**Ketching), a novel federated LoRA framework to enable effective updating of both low-rank adapters with robust differential privacy. Inspired by randomized SVD, our key idea is a two-stage sketching pipeline. This pipeline first aggregates carefully sketched, privacy-preserving local updates, and then reconstructs the global matrices on the server to facilitate effective updating of both adapters. We theoretically prove FedASK’s differential privacy guarantee and its exact aggregation property. Comprehensive experiments demonstrate that FedASK consistently outperforms baseline methods across a variety of privacy settings and data distributions. The code is available at <https://github.com/FLEECERmw/PrivacyFedLLM#>.

1 Introduction

Federated fine-tuning of Large Language Models (LLMs) presents a compelling paradigm for specializing these powerful models on domain-specific, distributed datasets without centralizing sensitive information [37, 23, 42]. However, the sheer scale of LLMs, often involving hundreds of

*equal contribution

†equal contribution

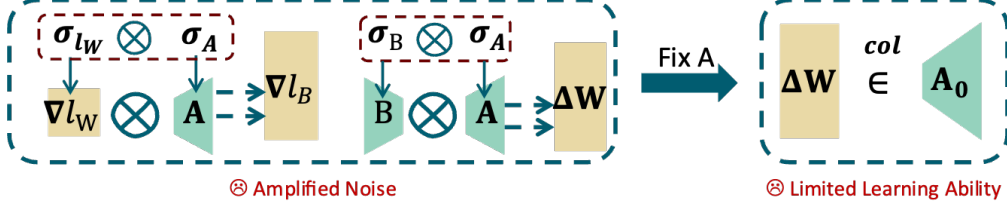


Figure 1: The *dilemma* of differential privacy with Federated LoRA: standard federated LoRA amplifies model noise, while fixing one adapter causes insufficient learnability.

billions of parameters, renders full-parameter fine-tuning prohibitive for local clients in FL due to severe memory, computation, and communication constraints [42]. To overcome these limitations, Parameter-Efficient Fine-Tuning (PEFT) methods, particularly Low-Rank Adaptation (LoRA) [19], have gained prominence [15]. LoRA facilitates efficient adaptation by freezing the pre-trained model weights W_0 and training only a small set of low-rank matrices, $A \in \mathbb{R}^{r \times n}$ and $B \in \mathbb{R}^{m \times r}$ (where $r \ll \min(m, n)$). The update $\Delta W = BA$ significantly reduces the number of trainable parameters, thereby alleviating the burdens of local processing and communication overhead in federated LLM fine-tuning scenarios.

Ensuring privacy in federated learning is critical, especially when fine-tuning LLMs [26]. The inherent scale and complexity of LLMs lead to greater probability of encoding and revealing sensitive information from training data compared to smaller models. While raw data are not shared in FL settings, the model updates and gradients transmitted can still potentially leak private client information. Therefore, providing robust privacy protection with theoretical guarantees is essential. Differential Privacy (DP) [8, 1] serves as a principled framework to achieve this, typically by introducing calibrated noise during the training process.

However, applying DP to federated LoRA presents a fundamental trade-off. On the one hand, achieving robust privacy often requires adding noise to the gradients of low-rank matrices A and B . Despite this, the intertwined nature of these gradients leads to significant noise amplification when both matrices are perturbed. This significantly increases the magnitude of noise in the resulting ΔW update, degrading the quality of the model update [31, 20]. On the other hand, existing methods commonly address this noise amplification by fixing one of the matrices (typically A) during training. Such strategies help mitigate the noise, particularly by avoiding the detrimental quadratic noise term. However, it fundamentally restricts the representational capacity of the LoRA parameters to a predetermined subspace, thereby impairing the model’s ability to adapt effectively [12, 41]. Motivated by this critical dilemma, this paper addresses the following research question: **Can we design a federated LoRA that achieves differential privacy guarantee, learnability, and communication efficiency simultaneously?**

To address this dilemma, we propose **FedASK** (Differentially Private **F**ederated Low Rank **A**daptation with Double **S**ketching). FedASK is the first federated LoRA framework designed to enable effective updates of both low-rank matrices under robust DP, overcoming the critical noise amplification and limited learnability trade-off inherent in prior methods. Our core insight is a novel two-stage projection pipeline, inspired by randomized SVD [14]. This pipeline achieves precise and resource-efficient aggregation of local LoRA update products, avoiding the issues of directly aggregating noisy matrices. Differential privacy is guaranteed by applying DP-SGD [1] with noise addition and clipping to local updates. Critically, the global SVD-based aggregation step is not merely an aggregation, but powerfully leverages this privatized information to influence and update both global matrices A and B , facilitating comprehensive adaptation capabilities under stringent DP constraints. Our key contributions are summarized as follows.

- We introduce FedASK, the first privacy preserving LoRA framework that updates both low-rank matrices, and achieves robust noise suppression, privacy guarantees, and resource-efficient operations.
- We theoretically prove the DP guarantee and the precise aggregation property of FedASK.
- FedASK empirically achieves consistent performance gains over state-of-the-art baselines in federated LLM fine-tuning, delivering up to an 11.5% performance improvement on MMLU (7B model) and a 46% improvement on GSM8K (13B model) under strong differential privacy.

Table 1: Federated LoRA Comparison. DP (\checkmark/\times): Supports DP. Agg. Type: Aggregation Precision. Client Init.: Parameter state before local training (Sync=Use Global Para, Keep B=Use Local B, Fixed A=Use Initial A, Rand A=Gaussian). " d_t " is the input feature dimension, and " r " is the LoRA rank.

METHOD	DP	AGG. TYPE	AGG. MEMORY	COMMUNICATION	CLIENT INIT.
FEDAVG	\times	IMPRECISE	$O(d_l r)$	$O(K d_l r)$	SYNC A, B
FLORA	\times	PRECISE	$O(d_l^2 + K d_l r)$	$O(K^2 d_l r)$	B = $\mathbf{0}$, $A_k^0 = \text{RAND}$
FEDSA	\times	IMPRECISE	$O(d_l r)$	$O(K d_l r)$	SYNC A, KEEP LOCAL B
FED-FFA	\checkmark	PRECISE	$O(d_l r)$	$O(K d_l r)$	FIX A, SYNC B
FEDASK	\checkmark	PRECISE	$O(d_l r)$	$O(K d_l r)$	SYNC A, B

2 Preliminary

In this section, we describe the background on LoRA fine-tuning of LLMs, particularly within the context of Federated Learning. We also introduce the concept of DP and its relevance to protecting client data.

2.1 Federated Learning with LoRA

The goal of Federated Learning with LoRA [36, 21, 39] is to minimize the global objective function:

$$F(W) = \frac{1}{K} \sum_{k=1}^K f_k(W_k, \mathcal{D}_k), \quad (1)$$

where $f_k(W_k, \mathcal{D}_k) = \frac{1}{|\mathcal{D}_k|} \sum_{\xi \in \mathcal{D}_k} l(W_k, \xi)$ represents the local objective function at client k . Here, W_k denotes the weight matrix of the local model, and \mathcal{D}_k is the local dataset at the client k . The function $l(W_k, \xi)$ computes the loss for a single data point $\xi \in \mathcal{D}_k$, and f_k averages this loss across the entire dataset. In LoRA, instead of directly training the full weight matrix W_k , we update it by adding a low-rank decomposition product to the pre-trained weights W_0 , and using gradient-based oracles to optimize the adapters.

$$\frac{\partial l}{\partial A_k} = \frac{\alpha}{r} B_k^T \frac{\partial l}{\partial W_k}, \quad \frac{\partial l}{\partial B_k} = \frac{\alpha}{r} \frac{\partial l}{\partial W_k} A_k^T, \quad (2)$$

where $A_k \in \mathbb{R}^{r \times n}$ and $B_k \in \mathbb{R}^{m \times r}$ are low-rank matrices with rank r (typically $r \ll \min(m, n)$), and α is a scaling factor. These matrices A_k and B_k are the parameters learned during fine-tuning.

A straightforward approach for Federated LoRA involves clients locally training their LoRA matrices (A_k and B_k) and then average them on the server [13, 25]. However, this direct averaging approach causes a misalignment with the precise global model update [34].

$$\bar{W} = \frac{1}{K} \sum_{k=1}^K W_k = \frac{1}{K} \sum_{k=1}^K (W_0 + \frac{\alpha}{r} B_k A_k) \neq W_0 + \frac{\alpha}{K^2 r} \sum_{k=1}^K B_k \sum_{k=1}^K A_k. \quad (3)$$

This discrepancy introduces undesirable cross-term noise, particularly in the presence of data heterogeneity across clients. Prior work [3, 31, 34] has recognized the same issue. Existing methods propose different strategies to address this misalignment. SLoRA [3] employs a multi-stage approach with sparse fine-tuning and SVD-based initialization, which incurs additional computational overhead. FFA-LoRA [31] adopts a simplified strategy by freezing matrix A and optimizing only B, limiting the model's expressive capability. FLoRA [34] relies on stacking and processing matrices on the server side, resulting in increased server computation and communication costs.

2.2 DP in Federated LoRA

We hereby define differential privacy as the following [9, 11]:

Definition 1. A randomized algorithm $\mathcal{M} : \mathcal{D} \rightarrow \mathcal{S}$ satisfies (ϵ, δ) -differential privacy if, for any two adjacent datasets $D, D' \in \mathcal{D}$ differing in one data point, and any output subset $S \subseteq \mathcal{S}$

$$\Pr[\mathcal{M}(D) \in S] \leq e^\epsilon \Pr[\mathcal{M}(D') \in S] + \delta,$$

where $\epsilon \geq 0$ controls the privacy loss and $0 < \delta < 1$ is the failure probability.

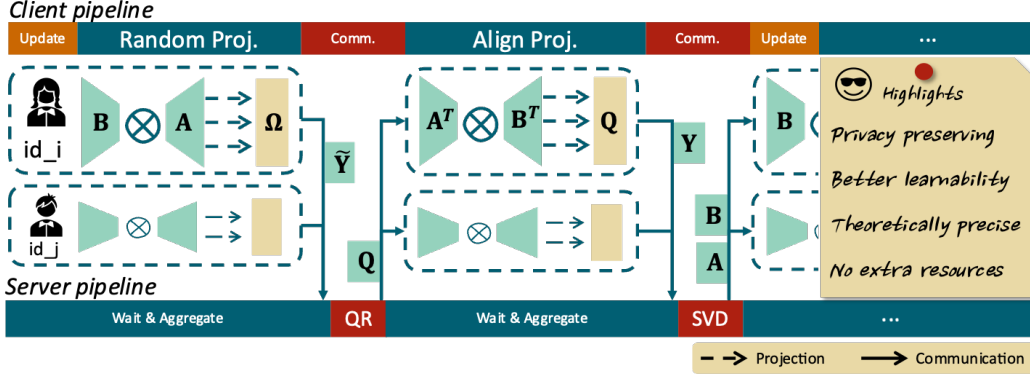


Figure 2: FedASK Pipeline.

DP theoretically ensures that this algorithm’s output is nearly unaffected by the presence or absence of any single individual’s data in the dataset. In the context of federated learning, DP is commonly achieved through DP-Stochastic Gradient Descent (DP-SGD)[1, 22]. This method adds calibrated noise to the gradients computed at each client before aggregation.

Applying DP-SGD directly to the standard LoRA update mechanism presents challenges. Specifically, when independent DP noise is added to the gradients of both A and B , these noise components interact quadratically during the construction of the LoRA update ΔW . This interaction leads to significant noise amplification, as detailed in Lemma 1. Existing strategies commonly mitigate this noise amplification by freezing one matrix and optimizing the other [31, 20]. This approach successfully avoids the quadratic noise term. However, since the parameter update is constrained to a specific subspace, it limits the model’s learning capability and hinders effective adaptation to the target task. Table 1 underscores FedASK’s distinct advantages over existing federated LoRA methods. Overcoming the adaptability limitations of fixed-matrix DP LoRA methods, FedASK enables dynamic and synchronized update of both LoRA matrices A and B under strong DP guarantees, achieving precise aggregation with resource efficiency comparable to or better than existing baselines.

3 FedASK Framework

This section presents FedASK (Differentially Private **F**ederated Low Rank Adaptation with Double **SK**etching) for federated fine-tuning of large language models using LoRA. We first introduce the overall FedASK framework, which contains the two-stage projection pipeline designed for efficient and precise global updates. Subsequently, we describe the integrated DP framework, which facilitates privacy-preserving training.

3.1 Pipeline: Two-Stage Sketching

The core innovation of FedASK lies in its efficient two-stage pipeline, which employs sketching and projection techniques to accurately compute the aggregated LoRA update ($\sum_k B_k A_k$) while minimizing resource overhead. FedASK is motivated by the observation that the weight updates in large neural networks [18, 2], particularly with methods like LoRA, exhibit a low-rank structure. This inherent property allows their essential information to be captured efficiently in a low-dimensional subspace.

Directly computing and aggregating the full product matrices $B_k A_k$ from each client would be computationally expensive and communication-heavy, as these matrices are of the same dimension as the original weight matrices adapted by LoRA. FedASK addresses the challenge by adopting sketching principles inspired by randomized SVD [14]. Clients transmit compressed representations instead of full matrices. Since the aggregated LoRA update also maintains a low-rank structure, these sketching techniques can effectively capture its essential information, enabling the server to perform a precise reconstruction. The overall process unfolds in two stages.

First stage: Randomized Subspace Sketching. Within the FedASK framework, local clients perform the standard LoRA training procedures to obtain their updated local matrices, denoted as B_k^t and A_k^t . To enable global aggregation, FedASK utilizes a shared random projection matrix

Algorithm 1 FedASK

Input: Initial global weight matrix \mathbf{W}_0 ; LoRA rank r ; LoRA scaling factor α ; Over-sketching parameter p ; Client learning rate γ ; Set of all clients \mathcal{K} ; Communication rounds T ; Local update steps m ; Boolean DP flag `use_DP`; Input feature dimension d_l .

Output: Final global LoRA matrices $\mathbf{A}^T, \mathbf{B}^T$.

Initialization:

Initialize $\mathbf{A}^0 \in \mathbb{R}^{r \times d_l}, \mathbf{B}^0 \in \mathbb{R}^{d_l \times r}$; Generate $\Omega \in \mathbb{R}^{d_l \times (r+p)}$.

for $t = 1$ **to** T **do**

Sample $\mathcal{K}_t \subseteq \mathcal{K}$; Broadcast $\mathbf{A}^{t-1}, \mathbf{B}^{t-1}, \Omega$ to clients in \mathcal{K}_t .

for each client $k \in \mathcal{K}_t$ **in parallel do**

if `use_DP` **is true then**

$\mathbf{A}_k^t \leftarrow \mathbf{A}^{t-1}, \mathbf{B}_k^t \leftarrow \text{LocalUpdate_DP}(\mathbf{B}^{t-1}, \mathbf{A}_k^t, \mathcal{D}_k, m, \gamma, \alpha)$

else

$\mathbf{A}_k^t, \mathbf{B}_k^t \leftarrow \text{LocalUpdate}(\mathbf{A}^{t-1}, \mathbf{B}^{t-1}, \mathcal{D}_k, m, \gamma, \alpha)$

end if

Compute $\mathbf{Y}_k^{proj} = \mathbf{B}_k^t(\mathbf{A}_k^t \Omega)$; Send to server.

end for

Aggregate $\mathbf{Y}_{agg}^t = \sum_{k \in \mathcal{K}_t} \mathbf{Y}_k^{proj}$; Perform QR: $\mathbf{Q}^t, _ = \text{QR}(\mathbf{Y}_{agg}^t)$.

Broadcast \mathbf{Q}^t to clients in \mathcal{K}_t .

for each client $k \in \mathcal{K}_t$ **in parallel do**

Compute $\tilde{\mathbf{Y}}_k^{proj} = (\mathbf{A}_k^t)^\top ((\mathbf{B}_k^t)^\top \mathbf{Q}^t)$; Send to server.

end for

Aggregate $\tilde{\mathbf{Y}}_{agg}^t = \sum_{k \in \mathcal{K}_t} \tilde{\mathbf{Y}}_k^{proj}$.

Compute SVD of $(\tilde{\mathbf{Y}}_{agg}^t)^\top$: $\mathbf{U}, \Sigma, \mathbf{V}^\top = \text{SVD}((\tilde{\mathbf{Y}}_{agg}^t)^\top)$.

Select leading r components $\mathbf{U}_r, \Sigma_r, \mathbf{V}_r^\top$.

Update global LoRA matrices: $\mathbf{B}^t \leftarrow \mathbf{Q}^t \mathbf{U}_r \Sigma_r^{\frac{1}{2}}$; $\mathbf{A}^t \leftarrow \Sigma_r^{\frac{1}{2}} \mathbf{V}_r^\top$

end for

$\Omega \in \mathbb{R}^{n \times (r+p)}$ to sketch these updated matrices. Specifically, each client computes the projection by:

$$\mathbf{Y}_k^{proj} = \mathbf{B}_k^t(\mathbf{A}_k^t \Omega). \quad (4)$$

Subsequently, this computed projection is transmitted to the server. The server aggregates these received projections and performs a QR decomposition to derive an orthonormal basis \mathbf{Q} , which is then redistributed to the participating clients. This basis serves to capture the global singular subspace relevant to the exact aggregated $\mathbf{B}^t \mathbf{A}^t$, helping to revise the random projection of the first stage and align the local parameter to the Global Space.

Second stage: Global Alignment Projection. After receiving the orthonormal basis \mathbf{Q} , the clients project their updated matrices onto this basis, yielding an updated projection:

$$\tilde{\mathbf{Y}}_k^{proj} = (\mathbf{A}_k^t)^\top ((\mathbf{B}_k^t)^\top \mathbf{Q}). \quad (5)$$

The server then aggregates these updated projections and proceeds to perform a Singular Value Decomposition (SVD) on the aggregated matrix to decompose it into its singular components. Finally, the global parameters \mathbf{A}^t and \mathbf{B}^t are updated based on the results of the SVD as follows:

$$\mathbf{B}^t = \mathbf{Q} \mathbf{U} \Sigma^{\frac{1}{2}}, \quad \mathbf{A}^t = \Sigma^{\frac{1}{2}} \mathbf{V}^\top. \quad (6)$$

This two-stage process enables FedASK to achieve a precise global update that is mathematically equivalent to the average of local updates $\frac{1}{K} \sum_k \mathbf{B}_k \mathbf{A}_k$ within a subspace rank $r + p$. The formal theoretical guarantee for this exact aggregation property is detailed within Section 4.

3.2 Differentially Private Local Updates in FedASK

To ensure the privacy of individual clients' sensitive data during the training process, we integrate Differential Privacy (DP) into our FedASK framework. As detailed in Algorithm 1, DP is applied conditionally based on the `use_DP` flag (line 6). When `use_DP` is set to true, each selected client $k \in \mathcal{K}_t$ executes the `LocalUpdate_DP` function (line 7). In the DP-enabled mode, the local update conducts on the \mathbf{B}_k matrix, while \mathbf{A}_k remains fixed for that local training phase ($\mathbf{A}_k^t \leftarrow \mathbf{A}^{t-1}$).

Within the `LocalUpdate_DP` function, the LoRA matrix \mathbf{B}_k is updated at each step τ using the DP-SGD mechanism. The process, incorporating gradient clipping and calibrated noise addition, is

formulated as:

$$B_k^{\tau+1} = B_k^\tau - \frac{\gamma\alpha}{r} \left(\frac{\partial l}{\partial W_k^\tau} / \max \left(1, \frac{\|\frac{\partial l}{\partial W_k^\tau}\|_2}{C} \right) + \mathcal{N}(0, \sigma^2 C^2 \mathbf{I}) \right) (A^{t-1})^T, \quad (7)$$

where γ and α denote the learning rate and the LoRA scaling factor, respectively.

Although A_k is not directly perturbed by local noise in DP rounds, the information learned and privatized via updates to B_k is not confined to global B^t . When the server aggregates the client projections and performs the SVD reconstruction, the resulting global factors A^t and B^t are both updated. The SVD step effectively decomposes the aggregated privatized information captured primarily within the B_k updates and redistributes it across *both* newly formed global matrices $A^t = \Sigma^{\frac{1}{2}} V^T$ and $B^t = U \Sigma^{\frac{1}{2}}$.

Therefore, FedASK's unique two-stage projection and SVD-based aggregation allow the knowledge gained under differential privacy to influence the global representation captured by A^t as well. The formal privacy analysis proving the (ϵ, δ) -guarantee for FedASK is presented in the following section.

4 Theoretical Analysis

This section highlights the theoretical analysis of FedASK, focusing on two key guarantees: robust differential privacy and precise aggregation.

4.1 Robust Differential Privacy Integration

Applying differential privacy to Low-Rank Adaptation (LoRA), particularly when simultaneously updating both low-rank matrices A_t and B_t through DP-SGD, presents a significant challenge. Lemma 1 provides a formal quantitative analysis of this noise amplification.

Lemma 1 (Approximate Noise Power in LoRA Update with DP-SGD). *Consider LoRA parameters $A_t \in \mathbb{R}^{r \times d_l}$ and $B_t \in \mathbb{R}^{d_l \times r}$ (where $d_l \gg r$). Under DP-SGD with learning rate η , noise multiplier σ , clipping C , and batch size B_{size} , independent Gaussian noises ξ_A, ξ_B (effective per-component variance $\sigma^2 C^2 / B_{size}^2$) are added to gradients $\nabla A_t, \nabla B_t$, respectively. Let ΔW_{noise} be the noise component of the resulting LoRA update.*

$$\mathbb{E}[\|\Delta W_{noise}\|_F^2] \approx \underbrace{\eta^2 \frac{\sigma^2 C^2}{B_{size}^2} d_l r (\|A_t\|_F^2 + \|B_t\|_F^2)}_{\text{Term 1: Linear Noise}} + \underbrace{\eta^4 \frac{\sigma^4 C^4}{B_{size}^4} d_l^2 r}_{\text{Term 2: Quadratic Noise}} + O(\eta^4 \sigma^2 + \eta^3 \sigma^2). \quad (8)$$

While Term 1 reflects standard linear noise as in DP-SGD, Term 2 arises from noise interaction and can dominate with large σ or η , scaling with d_l^2 . This causes the LoRA update's Signal-to-Noise Ratio (SNR) to degrade significantly faster ($1/\sigma^4$) than individual gradient SNRs ($1/\sigma^2$), revealing a critical noise amplification problem in standard DP-LoRA.

Lemma 1 highlights a critical challenge in standard DP-LoRA: simultaneously perturbing both low-rank matrices A_t and B_t leads to a dominant quadratic noise term, severely degrading the LoRA update's signal-to-noise ratio and impacting model utility. FedASK involves focusing local DP-SGD updates primarily on the B_k matrix, while A_k^t is primarily updated on the server through the two-stage aggregation pipeline with a global SVD-based update. This strategy preempts local generation of the problematic quadratic noise term. The formal (ϵ, δ) -differential privacy guarantee for FedASK is established in Theorem 1.

Theorem 1 (Privacy Guarantee of FedASK). *Suppose the gradient sensitivity is $C = 1$. FedASK (Algorithm 1) guarantees that the final global LoRA matrices (A^T, B^T) are (ϵ, δ) -differentially private with respect to the joint dataset $D = \bigcup_{i=1}^K \mathcal{D}_k$ of K total clients, provided the variance σ^2 of the Gaussian noise added to local gradients satisfies:*

$$\sigma^2 = O \left(\frac{q_D^2 \cdot m \cdot q_K \cdot T \cdot \ln(2/\delta) \cdot \ln(2T q_K / \delta)}{\epsilon^2 \cdot K} \right),$$

where q_K is the client sampling ratio per communication round (total T rounds), and q_D is the data sampling ratio per local update (total m local updates per client per round).

Theorem 1 establishes the end-to-end (ϵ, δ) -differential privacy for FedASK. Noise variance σ^2 scales consistent with established DP-SGD analyzes in federated learning [29]. The derivation rigorously tracks privacy loss using Rényi Differential Privacy (RDP), briefly with the following arguments. (1) Prove the RDP guarantee for two sketches Y_k^{proj} and $\tilde{Y}_k^{\text{proj}}$ released by a client k within a single communication round, relative to its local data \mathcal{D}_k ; (2) convert this per round, per client RDP into an intermediate (ϵ_0, δ_0) -DP guarantee; (3) applying advanced composition theorems for (ϵ, δ) -DP over T communication rounds; and (4) incorporate privacy amplification from client subsampling (ratio q_K) to achieve the final stated (ϵ, δ) -DP guarantee. The detailed proof is provided in Appendix A.2.

4.2 Aggregate Precision Guarantee

Aggregating local updates in federated LoRA presents a key challenge: achieving high accuracy while minimizing communication and computational overhead. Unlike conventional methods that may introduce approximation errors or require extensive resources (e.g., naive SVD reconstruction), FedASK’s two-stage sketching mechanism enables mathematically exact aggregation as formalized in theorem 2.

Theorem 2 (Aggregate Precision of FedASK). *Let $d_B = \dim(\text{span}(\bigcup_{k=1}^K \text{Range}(\mathbf{B}_k)))$. If the random projection matrix $\Omega \in \mathbb{R}^{n \times (r+p)}$ is a standard Gaussian random matrix with over-sketching parameter p satisfying $p \geq d_B - r + 2$, then FedASK guarantees that the global update before truncation $\Delta W^t = \mathbf{B}^t \mathbf{A}^t$ equals the exact average of local updates $\Delta \bar{W} = \frac{1}{K} \sum_{k=1}^K \mathbf{B}_k \mathbf{A}_k$, i.e.,*

$$\|\Delta W^t - \Delta \bar{W}\|_F = 0,$$

where $\|\cdot\|_F$ denotes the Frobenius norm.

Theorem 2 provides a theoretical guarantee: the global LoRA update (ΔW^t) computed by FedASK precisely matches the true average of all participating clients’ local updates ($\Delta \bar{W}$), provided the specified condition for the over-sketching parameter p is met. Our empirical evaluations (detailed in Section 5.3) suggest that this condition for exact, or near-exact, aggregation is often satisfied with a relatively small value for p . This implies that the theoretical precision highlighted by the theorem is practically achievable with minimal over-sketching overhead. Thus, FedASK delivers significant efficiency gains through its projection-based communication without compromising aggregation fidelity in practical settings.

5 Experiment

To rigorously evaluate our proposed method, experiments are conducted using two large-scale Llama-2 models: the 7B and 13B versions [32]. The Llama-2-7B model is fine-tuned on the dolly-15K dataset [40] and assessed on general language understanding benchmarks, including MMLU [16], DROP [7], and HumanEval [5]. Concurrently, the Llama-2-13B model undergoes further fine-tuning with Chain-of-Thought (CoT) prompting [35] on the MetaMathQA dataset [38], with its mathematical reasoning capabilities evaluated using GSM8K [6], GSM8K-hard, and MATH [17] benchmarks. Experimental conditions are systematically varied, encompassing different privacy budget levels (Section 5.1), varying degrees of data heterogeneity (Section 5.2), and an analysis of system efficiency (Section 5.3). All experiments are performed on NVIDIA Tesla A100 GPUs, utilizing half-precision to maximize computational efficiency.

Baselines. We compare FedASK with five baseline methods: (1) **FedAvg** [27]: Clients perform local SGD, and the server applies weighted parameter averaging. (2) **FFA-LoRA** [31]: Clients train one low-rank matrix locally, mitigating noise accumulation. (3) **FedSA-LoRA** [12]: Clients locally update both LoRA matrices, with one matrix being transmitted. (4) **FedProx** [24]: Introduces a proximal term in the local client loss to mitigate the effects of data heterogeneity. (5) **Scaffold** [30]: Employs control variates to correct client-server gradient disparities, reducing client drift.

5.1 Model Performance with Differential Privacy Guarantees

Experiments with the Llama-2-7B model focus on homogeneous data distributions. To ensure fair comparisons, standardized settings include a batch size \mathcal{B} of 8, 10 local update steps, and 4000 total communication rounds. Transformer-related hyperparameters, such as the sequence length l_{seq} of

Table 2: Performance Comparison of Different Algorithms with DP Budgets on Llama-2-7B.

Task	Priv. Budget	FedASK	FedAvg	FFA-LoRA	FedSA-LoRA	FedProx	Scaffold
MMLU	Non-Private	46.15	45.13	45.98	45.19	44.98	45.65
	$\epsilon = 1$	45.80	42.07	42.76	42.9	41.99	43.41
	$\epsilon = 3$	46.25	41.49	42.72	41.13	43.17	42.47
	$\epsilon = 6$	45.78	43.34	42.82	42.84	43.70	43.80
DROP	Non-Private	32.09	30.2	31.34	31.23	30.99	30.01
	$\epsilon = 1$	31.23	29.55	29.10	31.04	29.51	29.66
	$\epsilon = 3$	32.08	29.26	28.40	29.40	28.50	28.75
	$\epsilon = 6$	31.36	29.30	29.40	29.26	27.57	30.20
Human-Eval	Non-Private	15.24	11.59	14.02	12.2	12.2	14.63
	$\epsilon = 1$	15.24	12.80	12.20	13.41	12.20	9.76
	$\epsilon = 3$	15.24	10.37	10.98	10.98	13.41	11.59
	$\epsilon = 6$	15.85	11.59	12.20	12.80	10.98	12.20

Table 3: Performance Comparison of Different Algorithms with DP Budgets on Llama-2-13B.

Task	Priv. Budget	FedASK	FedAvg	FFA-LoRA	FedSA-LoRA	FedProx	Scaffold
GSM8K	Non-Private	50	48.5	48.4	47.2	47.8	45.6
	$\epsilon = 1$	22.7	15.5	14.2	12.2	15.2	16.1
	$\epsilon = 3$	24.8	16.5	20.0	20.2	18.0	15.8
	$\epsilon = 6$	27.7	19.3	20.2	17.3	20.1	20.3
GSM8K _{hard}	Non-Private	28.7	25.8	23.2	23.4	26.1	21.8
	$\epsilon = 1$	13.0	8.8	8.0	6.6	7.2	9.1
	$\epsilon = 3$	12.6	11.1	10.5	11.3	10.8	11.0
	$\epsilon = 6$	16.9	10.5	9.2	10.2	10.9	10.8
Math	Non-Private	11.8	10.3	10.8	10.7	11.7	9.8
	$\epsilon = 1$	6.9	5.2	5.8	5.6	5.6	5.8
	$\epsilon = 3$	6.6	6.1	6.0	5.9	6.4	5.5
	$\epsilon = 6$	7.6	6.2	6.0	5.9	6.7	7.1

128, align with previous studies [18]. The LoRA rank r is fixed at 64, with the scaling factor α set to twice the rank. Optimal performance is determined through a grid search over learning rates $\{5e-5, 1e-4, 2e-4, 5e-4\}$, and in differential privacy scenarios, privacy budgets $\epsilon \in \{1, 3, 6\}$ are explored, consistent with prior work [31]. Results are summarized in Table 2.

For the Llama-2-13B experiments, we use a batch size \mathcal{B} of 6, extend the total communication rounds to 8000, adjust the sequence length l_{seq} to 968, and increase the LoRA rank r to 128. Other settings remain the same as in the Llama-2-7B experiments. Results are summarized in Table 3.

The introduction of privacy-preserving mechanisms leads to performance degradation in several baseline methods. In contrast, our FedASK algorithm consistently outperforms these methods, regardless of whether privacy protection is enabled, demonstrating its superior generalization under privacy constraints. Interestingly, we find that under certain conditions, adding DP noise improves performance compared to the noiseless case. We attribute this to DP noise serving as implicit regularization, thereby enhancing model robustness.

5.2 Model Performance with Data Heterogeneity

To evaluate data heterogeneity’s impact, we experiment with IID and three non-IID scenarios, using 10 clients with 2 selected per round. In IID settings, data is randomly partitioned. For non-IID settings, we use Dirichlet distribution $\text{Dir}(\alpha)$ with $\alpha \in \{0.1, 0.5, 1.0\}$, following prior work [12]. To evaluate robustness under DP in these non-IID environments, we set the privacy budget $\epsilon = 3$, a common value for balancing privacy and utility. Other settings follow Section 5.1.

The experimental results in Table 4 demonstrate FedASK’s prominent performance. Across all tasks and data distributions (IID and non-IID), FedASK consistently outperforms baselines, underscoring its effectiveness and robustness. This superior performance stems from FedASK’s simultaneous local updates and global aggregation of both A and B matrices. While previous research [12] suggests that

matrix A learns global information and matrix B captures local specifics, FedASK’s design enables a continuous interaction and fusion of these distinct knowledge types. This inherent information fusion capability enhances the model’s adaptation to heterogeneous data distributions.

Table 4: Performance comparison across different data distributions on various tasks.

Task	Data Dist.	FedASK	FedAvg	FFA-LoRA	FedSA-LoRA	FedProx	Scaffold
MMLU	IID	46.25	41.49	42.72	41.13	43.17	42.47
	Dir(0.1)	46.04	42.69	42.54	44.27	42.61	43.05
	Dir(0.5)	45.95	42.11	41.46	42.72	42.98	41.97
	Dir(1)	46.01	42.96	43.23	41.04	42.98	41.71
DROP	IID	32.08	29.44	28.40	29.40	28.50	28.75
	Dir(0.1)	31.01	28.34	30.10	28.58	28.18	28.27
	Dir(0.5)	31.15	29.18	29.26	27.83	28.23	29.45
	Dir(1)	31.58	30.02	28.93	29.29	29.82	30.52
Human-Eval	IID	15.24	10.37	10.98	10.98	13.41	11.59
	Dir(0.1)	13.41	7.32	10.98	12.8	13.41	7.93
	Dir(0.5)	14.63	10.98	13.41	12.8	14.63	9.76
	Dir(1)	14.02	9.76	10.98	10.37	10.37	9.15

5.3 Effect of the Sketching Dimension

Theorem 2 provides a theoretical guarantee that FedASK achieves precise global aggregation provided the over-sketching parameter p meets a specified condition, our empirical evaluations aim to demonstrate that this precision is practically attainable with minimal p , underscoring FedASK’s efficiency. To this end, we conduct two sets of experiments using the Llama-2-7B model and identical settings from Section 5.1 to assess p ’s impact on both downstream task performance and direct aggregation fidelity.

First, to evaluate downstream task performance, we test FedASK with varying over-sketching parameters $p \in \{0, 32, 64, 96, 128\}$ on the MMLU benchmark. This is performed under a challenging Non-IID setting ($\alpha = 0.1$) with differential privacy ($\epsilon = 3$). Second, to directly assess aggregation fidelity, we compare FedASK configured with no over-sketching ($p = 0$) against FedAvg. This latter experiment is conducted without DP, across varying numbers of selected clients ($K_s \in \{2, 5, 10, 15, 20\}$) and data heterogeneity levels. After 30 local update rounds by each client, we measure aggregation fidelity using the cosine similarity between FedASK’s reconstructed global LoRA update ($\Delta W^t = B^t A^t$) and the ideal average of all the local LoRA updates ($\Delta \bar{W}^t = \frac{1}{K_s} \sum_{k \in K_s} B_k^t A_k^t$).

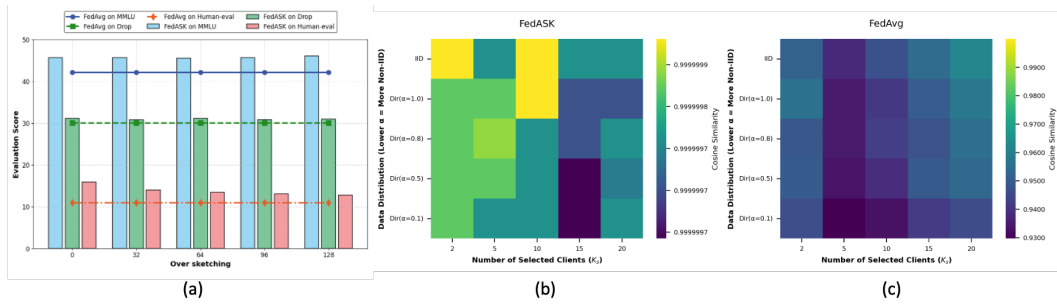


Figure 3: Impact of over-sketching p on FedASK. (a) MMLU score of FedASK versus p . (b) Aggregation fidelity of FedASK (with $p = 0$) and (c) FedAvg, measured by cosine similarity with the ideal mean of local updates (1.0 indicates perfect fidelity). Subplots (b) and (c) vary selected clients (K_s) and Non-IID degrees.

The empirical results, presented in Figure 3, illustrate that the over-sketching parameter p has a minimal influence on the effectiveness of FedASK. Firstly, (a) shows that FedASK’s MMLU performance remains remarkably stable across the tested p values (ranging from 45.63 at $p = 0$ to 46.06 at $p = 128$), even under conditions of significant data heterogeneity and differential privacy. This stability demonstrates a low sensitivity to p to achieve robust downstream utility. Secondly, FedASK’s inherent design ensures exceptional aggregation fidelity, even with zero over-sketching ($p = 0$). As shown in (b), FedASK consistently achieves near-perfect cosine similarities (with an

error on the order of 10^{-7}) across a variety of selected clients (K_s) and Non-IID degrees. This performance consistently outperforms FedAvg, presented in (c), which typically ranges from 0.92 to 0.96. These findings affirm FedASK’s practical efficiency and the attainability of its theoretically guaranteed precise aggregation with negligible over-sketching overhead.

6 Conclusion

This paper introduces FedASK, a novel federated LoRA framework that successfully resolves the trade-off between noise amplification and learnability in private federated fine-tuning. By employing a two-stage sketching pipeline, FedASK enables the differentially private and effective update of both LoRA adapters. Our theoretical analysis and comprehensive experiments demonstrate FedASK’s superior performance in achieving precise aggregation and robust downstream utility with strong privacy guarantees and practical efficiency. Future studies will focus on extending its applicability to a broader range of model architectures and complex training tasks, as well as exploring further refinements to its privacy-utility trade-off.

References

- [1] M. Abadi, A. Chu, I. Goodfellow, H. B. McMahan, I. Mironov, K. Talwar, and L. Zhang. Deep learning with differential privacy. In *Proceedings of the 2016 ACM SIGSAC Conference on Computer and Communications Security, CCS '16*, page 308–318, New York, NY, USA, 2016. Association for Computing Machinery. ISBN 9781450341394. doi: 10.1145/2976749.2978318. URL <https://doi.org/10.1145/2976749.2978318>.
- [2] A. Aghajanyan, L. Zettlemoyer, and S. Gupta. Intrinsic dimensionality explains the effectiveness of language model fine-tuning, 2020. URL <https://arxiv.org/abs/2012.13255>.
- [3] S. Babakniya, A. R. Elkordy, Y. H. Ezzeldin, Q. Liu, K.-B. Song, M. El-Khamy, and S. Avestimehr. Slora: Federated parameter efficient fine-tuning of language models, 2023. URL <https://arxiv.org/abs/2308.06522>.
- [4] B. Balle, G. Barthe, M. Gaboardi, J. Hsu, and T. Sato. Hypothesis testing interpretations and renyi differential privacy. In S. Chiappa and R. Calandra, editors, *Proceedings of the Twenty Third International Conference on Artificial Intelligence and Statistics*, volume 108 of *Proceedings of Machine Learning Research*, pages 2496–2506. PMLR, 26–28 Aug 2020. URL <https://proceedings.mlr.press/v108/balle20a.html>.
- [5] M. Chen, J. Tworek, H. Jun, Q. Yuan, H. Ponde de Oliveira Pinto, J. Kaplan, H. Edwards, et al. Evaluating Large Language Models Trained on Code. *arXiv e-prints*, art. arXiv:2107.03374, July 2021. doi: 10.48550/arXiv.2107.03374.
- [6] K. Cobbe, V. Kosaraju, M. Bavarian, M. Chen, H. Jun, L. Kaiser, M. Plappert, J. Tworek, J. Hilton, R. Nakano, C. Hesse, and J. Schulman. Training Verifiers to Solve Math Word Problems. *arXiv e-prints*, art. arXiv:2110.14168, Oct. 2021. doi: 10.48550/arXiv.2110.14168.
- [7] D. Dua, Y. Wang, P. Dasigi, G. Stanovsky, S. Singh, and M. Gardner. DROP: A Reading Comprehension Benchmark Requiring Discrete Reasoning Over Paragraphs. *arXiv e-prints*, art. arXiv:1903.00161, Mar. 2019. doi: 10.48550/arXiv.1903.00161.
- [8] C. Dwork. Differential privacy. In M. Bugliesi, B. Preneel, V. Sassone, and I. Wegener, editors, *Automata, Languages and Programming*, pages 1–12, Berlin, Heidelberg, 2006. Springer Berlin Heidelberg. ISBN 978-3-540-35908-1.
- [9] C. Dwork and A. Roth. The algorithmic foundations of differential privacy. *Foundations and Trends® in Theoretical Computer Science*, 9(3–4):211–407, 2014. ISSN 1551-305X. doi: 10.1561/04000000042. URL <http://dx.doi.org/10.1561/04000000042>.
- [10] C. Dwork, G. N. Rothblum, and S. Vadhan. Boosting and differential privacy. In *2010 IEEE 51st Annual Symposium on Foundations of Computer Science*, pages 51–60, 2010. doi: 10.1109/FOCS.2010.12.
- [11] J. Fu, Y. Hong, X. Ling, L. Wang, X. Ran, Z. Sun, W. H. Wang, Z. Chen, and Y. Cao. Differentially private federated learning: A systematic review. *arXiv preprint arXiv:2405.08299*, 2024.
- [12] P. Guo, S. Zeng, Y. Wang, H. Fan, F. Wang, and L. Qu. Selective aggregation for low-rank adaptation in federated learning, 2025. URL <https://arxiv.org/abs/2410.01463>.

- [13] Z. Guo, Y. Zhang, Z. Zhang, Z. Xu, and I. King. FedLFC: Towards efficient federated multilingual modeling with LoRA-based language family clustering. In K. Duh, H. Gomez, and S. Bethard, editors, *Findings of the Association for Computational Linguistics: NAACL 2024*, pages 1519–1528, Mexico City, Mexico, June 2024. Association for Computational Linguistics. doi: 10.18653/v1/2024.findings-naacl.98. URL <https://aclanthology.org/2024.findings-naacl.98/>.
- [14] N. Halko, P. G. Martinsson, and J. A. Tropp. Finding structure with randomness: Probabilistic algorithms for constructing approximate matrix decompositions. *SIAM Review*, 53(2):217–288, 2011. doi: 10.1137/090771806. URL <https://doi.org/10.1137/090771806>.
- [15] Z. Han, C. Gao, J. Liu, J. Zhang, and S. Q. Zhang. Parameter-efficient fine-tuning for large models: A comprehensive survey, 2024. URL <https://arxiv.org/abs/2403.14608>.
- [16] D. Hendrycks, C. Burns, S. Basart, A. Zou, M. Mazeika, D. Song, and J. Steinhardt. Measuring Massive Multitask Language Understanding. *arXiv e-prints*, art. arXiv:2009.03300, Sept. 2020. doi: 10.48550/arXiv.2009.03300.
- [17] D. Hendrycks, C. Burns, S. Kadavath, A. Arora, S. Basart, E. Tang, D. Song, and J. Steinhardt. Measuring Mathematical Problem Solving With the MATH Dataset. *arXiv e-prints*, art. arXiv:2103.03874, Mar. 2021. doi: 10.48550/arXiv.2103.03874.
- [18] E. J. Hu, Y. Shen, P. Wallis, Z. Allen-Zhu, Y. Li, S. Wang, L. Wang, and W. Chen. LoRA: Low-Rank Adaptation of Large Language Models. *arXiv e-prints*, art. arXiv:2106.09685, June 2021. doi: 10.48550/arXiv.2106.09685.
- [19] E. J. Hu, Y. Shen, P. Wallis, Z. Allen-Zhu, Y. Li, S. Wang, L. Wang, W. Chen, et al. Lora: Low-rank adaptation of large language models. *ICLR*, 1(2):3, 2022.
- [20] T. Kang, Z. Wang, H. He, J. Zhang, S. Song, and K. B. Letaief. Federated low-rank adaptation with differential privacy over wireless networks, 2024. URL <https://arxiv.org/abs/2411.07806>.
- [21] W. Kuang, B. Qian, Z. Li, D. Chen, D. Gao, X. Pan, Y. Xie, Y. Li, B. Ding, and J. Zhou. Federatedscope-llm: A comprehensive package for fine-tuning large language models in federated learning. In *Proceedings of the 30th ACM SIGKDD Conference on Knowledge Discovery and Data Mining, KDD '24*, page 5260–5271, New York, NY, USA, 2024. Association for Computing Machinery. ISBN 9798400704901. doi: 10.1145/3637528.3671573. URL <https://doi.org/10.1145/3637528.3671573>.
- [22] J. Lee and D. Kifer. Concentrated differentially private gradient descent with adaptive per-iteration privacy budget. In *Proceedings of the 24th ACM SIGKDD International Conference on Knowledge Discovery & Data Mining, KDD '18*, page 1656–1665, New York, NY, USA, 2018. Association for Computing Machinery. ISBN 9781450355520. doi: 10.1145/3219819.3220076. URL <https://doi.org/10.1145/3219819.3220076>.
- [23] T. Li, A. K. Sahu, A. Talwalkar, and V. Smith. Federated learning: Challenges, methods, and future directions. *IEEE Signal Processing Magazine*, 37(3):50–60, 2020. doi: 10.1109/MSP.2020.2975749.
- [24] T. Li, A. K. Sahu, M. Zaheer, M. Sanjabi, A. Talwalkar, and V. Smith. Federated optimization in heterogeneous networks. In I. Dhillon, D. Papailiopoulos, and V. Sze, editors, *Proceedings of Machine Learning and Systems*, volume 2, pages 429–450, 2020. URL https://proceedings.mlsys.org/paper_files/paper/2020/file/1f5fe83998a09396ebe6477d9475ba0c-Paper.pdf.
- [25] X.-Y. Liu, R. Zhu, D. Zha, J. Gao, S. Zhong, M. White, and M. Qiu. Differentially private low-rank adaptation of large language model using federated learning. *ACM Trans. Manage. Inf. Syst.*, 16(2), Mar. 2025. ISSN 2158-656X. doi: 10.1145/3682068. URL <https://doi.org/10.1145/3682068>.
- [26] N. Lukas, A. Salem, R. Sim, S. Tople, L. Wutschitz, and S. Zanella-Béguelin. Analyzing leakage of personally identifiable information in language models. In *2023 IEEE Symposium on Security and Privacy (SP)*, pages 346–363, 2023. doi: 10.1109/SP46215.2023.10179300.
- [27] H. B. McMahan, E. Moore, D. Ramage, S. Hampson, and B. Agüera y Arcas. Communication-Efficient Learning of Deep Networks from Decentralized Data. *arXiv e-prints*, art. arXiv:1602.05629, Feb. 2016. doi: 10.48550/arXiv.1602.05629.
- [28] I. Mironov. Rényi differential privacy. In *2017 IEEE 30th Computer Security Foundations Symposium (CSF)*, pages 263–275, 2017. doi: 10.1109/CSF.2017.11.

- [29] M. Noble, A. Bellet, and A. Dieuleveut. Differentially private federated learning on heterogeneous data. In G. Camps-Valls, F. J. R. Ruiz, and I. Valera, editors, *Proceedings of The 25th International Conference on Artificial Intelligence and Statistics*, volume 151 of *Proceedings of Machine Learning Research*, pages 10110–10145. PMLR, 28–30 Mar 2022. URL <https://proceedings.mlr.press/v151/noble22a.html>.
- [30] S. Praneeth Karimireddy, S. Kale, M. Mohri, S. J. Reddi, S. U. Stich, and A. Theertha Suresh. SCAFFOLD: Stochastic Controlled Averaging for Federated Learning. *arXiv e-prints*, art. arXiv:1910.06378, Oct. 2019. doi: 10.48550/arXiv.1910.06378.
- [31] Y. Sun, Z. Li, Y. Li, and B. Ding. Improving lora in privacy-preserving federated learning, 2024. URL <https://arxiv.org/abs/2403.12313>.
- [32] H. Touvron, L. Martin, K. Stone, P. Albert, A. Almahairi, Y. Babaei, N. Bashlykov, S. Batra, P. Bhargava, S. Bhosale, et al. Llama 2: Open foundation and fine-tuned chat models, 2023. URL <https://arxiv.org/abs/2307.09288>.
- [33] Y.-X. Wang, B. Balle, and S. P. Kasiviswanathan. Subsampled renyi differential privacy and analytical moments accountant. In K. Chaudhuri and M. Sugiyama, editors, *Proceedings of the Twenty-Second International Conference on Artificial Intelligence and Statistics*, volume 89 of *Proceedings of Machine Learning Research*, pages 1226–1235. PMLR, 16–18 Apr 2019. URL <https://proceedings.mlr.press/v89/wang19b.html>.
- [34] Z. Wang, Z. Shen, Y. He, G. Sun, H. Wang, L. Lyu, and A. Li. Flora: Federated fine-tuning large language models with heterogeneous low-rank adaptations, 2024. URL <https://arxiv.org/abs/2409.05976>.
- [35] J. Wei, X. Wang, D. Schuurmans, M. Bosma, B. Ichter, F. Xia, E. Chi, Q. Le, and D. Zhou. Chain-of-Thought Prompting Elicits Reasoning in Large Language Models. *arXiv e-prints*, art. arXiv:2201.11903, Jan. 2022. doi: 10.48550/arXiv.2201.11903.
- [36] R. Ye, W. Wang, J. Chai, D. Li, Z. Li, Y. Xu, Y. Du, Y. Wang, and S. Chen. Openfedllm: Training large language models on decentralized private data via federated learning. In *Proceedings of the 30th ACM SIGKDD Conference on Knowledge Discovery and Data Mining, KDD ’24*, page 6137–6147, New York, NY, USA, 2024. Association for Computing Machinery. ISBN 9798400704901. doi: 10.1145/3637528.3671582. URL <https://doi.org/10.1145/3637528.3671582>.
- [37] X. Yin, Y. Zhu, and J. Hu. A comprehensive survey of privacy-preserving federated learning: A taxonomy, review, and future directions. *ACM Comput. Surv.*, 54(6), July 2021. ISSN 0360-0300. doi: 10.1145/3460427. URL <https://doi.org/10.1145/3460427>.
- [38] L. Yu, W. Jiang, H. Shi, J. Yu, Z. Liu, Y. Zhang, J. T. Kwok, Z. Li, A. Weller, and W. Liu. MetaMath: Bootstrap Your Own Mathematical Questions for Large Language Models. *arXiv e-prints*, art. arXiv:2309.12284, Sept. 2023. doi: 10.48550/arXiv.2309.12284.
- [39] J. Zhang, S. Vahidian, M. Kuo, C. Li, R. Zhang, T. Yu, G. Wang, and Y. Chen. Towards building the federatedgpt: Federated instruction tuning. In *ICASSP 2024 - 2024 IEEE International Conference on Acoustics, Speech and Signal Processing (ICASSP)*, pages 6915–6919, 2024. doi: 10.1109/ICASSP48485.2024.10447454.
- [40] J. Zhang, S. Vahidian, M. Kuo, C. Li, R. Zhang, T. Yu, Y. Zhou, G. Wang, and Y. Chen. Towards building the federated gpt: Federated instruction tuning, 2024. URL <https://arxiv.org/abs/2305.05644>.
- [41] L. Zhang, L. Zhang, S. Shi, X. Chu, and B. Li. LoRA-FA: Memory-efficient low-rank adaptation for large language models fine-tuning, 2024. URL <https://openreview.net/forum?id=RbKThNNFxr>.
- [42] S. Zhang, L. Dong, X. Li, S. Zhang, X. Sun, S. Wang, J. Li, R. Hu, T. Zhang, F. Wu, and G. Wang. Instruction tuning for large language models: A survey, 2024. URL <https://arxiv.org/abs/2308.10792>.

A Theoretical Proof

A.1 Proof of Lemma 1

Proof. Let $A_t \in \mathbb{R}^{r \times d_l}$ and $B_t \in \mathbb{R}^{d_l \times r}$ be the LoRA matrices. The noisy updates under DP-SGD with learning rate η are,

$$A_{t+1} = A_t - \eta(\nabla A_t + \xi_A), \quad (9)$$

$$B_{t+1} = B_t - \eta(\nabla B_t + \xi_B), \quad (10)$$

where ξ_A, ξ_B are independent Gaussian noise matrices with i.i.d. entries $\mathcal{N}(0, \sigma_{eff}^2)$, and $\sigma_{eff}^2 = \sigma^2 C^2 / B_{size}^2$. The noise component in the LoRA update $\Delta W = B_{t+1}A_{t+1} - B_t A_t$ is found by substituting (9) and (10),

$$\begin{aligned}\Delta W &= (B_t - \eta(\nabla B_t + \xi_B))(A_t - \eta(\nabla A_t + \xi_A)) - B_t A_t, \\ &= -\eta(B_t \nabla A_t + \nabla B_t A_t) + \eta^2 \nabla B_t \nabla A_t \quad (\text{Signal part}) \\ &\quad - \eta(B_t \xi_A + \xi_B A_t) + \eta^2 (\nabla B_t \xi_A + \xi_B \nabla A_t + \xi_B \xi_A) \quad (\text{Noise part}).\end{aligned}$$

Thus, $\Delta W_{noise} = X + Y$, where,

$$X = -\eta(B_t \xi_A + \xi_B A_t), \quad (11)$$

$$Y = \eta^2 (\nabla B_t \xi_A + \xi_B \nabla A_t + \xi_B \xi_A). \quad (12)$$

The expected noise power is $P_N = \mathbb{E}[\|X + Y\|_F^2] = \mathbb{E}[\|X\|_F^2] + \mathbb{E}[\|Y\|_F^2] + 2\mathbb{E}[\langle X, Y \rangle_F]$.

For the linear noise term power $\mathbb{E}[\|X\|_F^2]$, using (11),

$$\begin{aligned}\mathbb{E}[\|X\|_F^2] &= \eta^2 \mathbb{E}[\|B_t \xi_A + \xi_B A_t\|_F^2], \\ &= \eta^2 (\mathbb{E}[\|B_t \xi_A\|_F^2] + \mathbb{E}[\|\xi_B A_t\|_F^2]),\end{aligned}$$

due to $\mathbb{E}[\langle B_t \xi_A, \xi_B A_t \rangle_F] = 0$ from noise independence and zero mean. We have $\mathbb{E}[\xi_A \xi_A^T] = d_l \sigma_{eff}^2 I_r$ and $\mathbb{E}[\xi_B^T \xi_B] = d_l \sigma_{eff}^2 I_r$. So,

$$\begin{aligned}\mathbb{E}[\|B_t \xi_A\|_F^2] &= \text{Tr}(B_t \mathbb{E}[\xi_A \xi_A^T] B_t^T) = d_l \sigma_{eff}^2 \|B_t\|_F^2, \\ \mathbb{E}[\|\xi_B A_t\|_F^2] &= \text{Tr}(A_t A_t^T \mathbb{E}[\xi_B^T \xi_B]) = d_l \sigma_{eff}^2 \|A_t\|_F^2.\end{aligned}$$

This yields,

$$\mathbb{E}[\|X\|_F^2] = \eta^2 d_l \sigma_{eff}^2 (\|A_t\|_F^2 + \|B_t\|_F^2). \quad (13)$$

For the cross term $2\mathbb{E}[\langle X, Y \rangle_F]$, using (11) and (12),

$$\mathbb{E}[\langle X, Y \rangle_F] = -\eta^3 \mathbb{E}[\langle B_t \xi_A + \xi_B A_t, \nabla B_t \xi_A + \xi_B \nabla A_t + \xi_B \xi_A \rangle_F].$$

Non-zero expectations arise from,

$$\begin{aligned}\mathbb{E}[\langle B_t \xi_A, \nabla B_t \xi_A \rangle_F] &= \text{Tr}(B_t^T \nabla B_t \mathbb{E}[\xi_A \xi_A^T]) = d_l \sigma_{eff}^2 \text{Tr}(B_t^T \nabla B_t), \\ \mathbb{E}[\langle \xi_B A_t, \xi_B \nabla A_t \rangle_F] &= \text{Tr}(A_t^T \mathbb{E}[\xi_B^T \xi_B] \nabla A_t) = d_l \sigma_{eff}^2 \text{Tr}(A_t^T \nabla A_t).\end{aligned}$$

Other terms are zero since the independence of noise. Thus,

$$2\mathbb{E}[\langle X, Y \rangle_F] = -2\eta^3 d_l \sigma_{eff}^2 (\text{Tr}(B_t^T \nabla B_t) + \text{Tr}(A_t^T \nabla A_t)). \quad (14)$$

For the higher-order noise term power $\mathbb{E}[\|Y\|_F^2]$, using (12), the dominant component is,

$$\mathbb{E}[\|\eta^2 \xi_B \xi_A\|_F^2] = \eta^4 \mathbb{E}[\text{Tr}(\xi_B \xi_A \xi_A^T \xi_B^T)], \quad (15)$$

$$= \eta^4 \text{Tr}(\mathbb{E}[\xi_B \mathbb{E}[\xi_A \xi_A^T] \xi_B^T]), \quad (16)$$

$$= \eta^4 \text{Tr}(\mathbb{E}[\xi_B (d_l \sigma_{eff}^2 I_r) \xi_B^T]), \quad (17)$$

$$= \eta^4 d_l \sigma_{eff}^2 \mathbb{E}[\|\xi_B\|_F^2] = \eta^4 d_l^2 r (\sigma_{eff}^2)^2. \quad (18)$$

Other terms in $\mathbb{E}[\|Y\|_F^2]$ are $O(\eta^4 \sigma_{eff}^2 d_l r (\|\nabla A_t\|_F^2 + \|\nabla B_t\|_F^2))$.

Combining the dominant terms from (13) and the dominant part of $\mathbb{E}[\|Y\|_F^2]$ (derived in (18)), and noting the cross-term (14) is often less dominant, we approximate P_N . Substituting $\sigma_{eff}^2 = \sigma^2 C^2 / B_{size}^2$, we get,

$$\mathbb{E}[\|\Delta W_{noise}\|_F^2] \approx \eta^2 \frac{\sigma^2 C^2}{B_{size}^2} d_l r (\|A_t\|_F^2 + \|B_t\|_F^2) + \eta^4 \frac{\sigma^4 C^4}{B_{size}^4} d_l^2 r, \quad (19)$$

which matches the expression stated in Lemma 1, highlighting the linear and dominant quadratic noise terms. \square

A.2 Proof of Theorem 1

To facilitate the privacy analysis of FedASK, we first recall several fundamental concepts and properties of differential privacy. We leverage the advanced composition theorem and subsampling theorem for (ϵ, δ) -differential privacy:

Lemma 2 (Advanced Composition [10]). *Let M_1, \dots, M_k be a sequence of k adaptive mechanisms, where each M_i provides (ϵ, δ) -differential privacy. For any $\delta' > 0$, the composed mechanism $M = (M_1, \dots, M_k)$ is $(\epsilon_{total}, k\delta + \delta')$ -differentially private, where*

$$\epsilon_{total} = \sqrt{2k \ln(1/\delta')} \epsilon + k\epsilon(e^\epsilon - 1).$$

If $\epsilon \ll 1$, then for any $\delta' > 0$, the composed mechanism M is $(\epsilon'_{total}, k\delta + \delta')$ -differentially private, where $\epsilon'_{total} \approx \sqrt{2k \ln(1/\delta')} \epsilon + k\epsilon^2$.

Lemma 3 (Privacy Amplification by Subsampling [33]). *Let \mathcal{M} be an (ϵ, δ) -differentially private mechanism. If \mathcal{M} is run on a random sample of size m drawn uniformly without replacement from a dataset of size N (where $m \leq N$), let $\gamma = m/N$ be the sampling ratio. Then, the subsampled mechanism $\mathcal{M}_{\text{subsample}}$ is (ϵ', δ') -differentially private, where,*

$$\begin{aligned} \epsilon' &= \log(1 + \gamma(e^\epsilon - 1)), \\ \delta' &= \gamma\delta. \end{aligned}$$

While (ϵ, δ) -DP provides a worst-case privacy guarantee, analyzing the precise privacy loss under composition, especially for Gaussian mechanisms, can be complex. Rényi Differential Privacy (RDP) [28] offers a convenient framework for tracking privacy loss, providing tighter bounds under composition. We define RDP as follows:

Definition 2 (RDP [28]). *A randomized mechanism $\mathcal{M} : \mathcal{D} \rightarrow \mathcal{R}$ satisfies (α, R) -Rényi Differential Privacy (RDP) if for any neighboring datasets $D, D' \in \mathcal{D}$ (differing in one individual's data), and for all $\alpha > 1$,*

$$D_\alpha(\mathcal{M}(D) || \mathcal{M}(D')) \leq R,$$

where $D_\alpha(P || Q) = \frac{1}{\alpha-1} \ln \mathbb{E}_{x \sim Q(x)} \left[\left(\frac{P(x)}{Q(x)} \right)^\alpha \right]$ is the Rényi divergence of order α .

RDP possesses several useful properties that simplify privacy analysis.

Lemma 4 (Post-processing of RDP [28]). *Let $\mathcal{M} : \mathcal{D} \rightarrow \mathcal{R}$ be a mechanism that satisfies (α, R) -RDP. Let $g : \mathcal{R} \rightarrow \mathcal{R}'$ be an arbitrary randomized mapping (a post-processing function). Then the mechanism $g \circ \mathcal{M} : \mathcal{D} \rightarrow \mathcal{R}'$ also satisfies (α, R) -RDP.*

Lemma 5 (Adaptive Sequential Composition of RDP [28]). *Let $\mathcal{M}_1 : \mathcal{D} \rightarrow \mathcal{R}_1$ be a mechanism satisfying (α, R_1) -RDP. Let $\mathcal{M}_2 : \mathcal{R}_1 \times \mathcal{D} \rightarrow \mathcal{R}_2$ be a mechanism such that for any fixed output $o_1 \in \mathcal{R}_1$ of \mathcal{M}_1 , $\mathcal{M}_2(o_1, \cdot)$ satisfies (α, R_2) -RDP. Then the mechanism $\mathcal{M}(D) = (\mathcal{M}_1(D), \mathcal{M}_2(\mathcal{M}_1(D), D))$, which outputs the pair (o_1, o_2) where $o_1 \sim \mathcal{M}_1(D)$ and $o_2 \sim \mathcal{M}_2(o_1, D)$, satisfies $(\alpha, R_1 + R_2)$ -RDP.*

Lemma 6 (Conversion from RDP to (ϵ, δ) -DP [4]). *If a randomized mechanism \mathcal{M} satisfies (α, R) -RDP, then it satisfies $(R + \ln((\alpha - 1)/\alpha) - (\ln \delta + \ln \alpha)/(\alpha - 1), \delta)$ -DP for any $0 < \delta < 1$.*

The core mechanism for achieving privacy in FedASK involves adding Gaussian noise. The RDP of a (subsampled) Gaussian mechanism is characterized as follows:

Lemma 7 (Approximate RDP for $q_{\mathcal{D}}$ -Subsampled Gaussian Mechanism [29]). *Consider a $q_{\mathcal{D}}$ -subsampled Gaussian mechanism with noise variance σ_g^2 . Under the assumption that the data subsampling ratio $q_{\mathcal{D}}$ is small (i.e., $q_{\mathcal{D}} = o(1)$), and assuming the mechanism operates in a high privacy regime (Assumption 1-(iii) in [29]), for any real number $\alpha > 1$, the mechanism satisfies (α, R') -RDP, where $R' = \mathcal{O}(\frac{q_{\mathcal{D}}^2(\alpha+1)}{\sigma_g^2})$.*

Proof. The proof proceeds in several steps. We first analyze the RDP guarantee for the information transmitted by a single client k in one communication round t with respect to its local dataset \mathcal{D}_k .

Then, we analyze the RDP of the aggregated global update at the server. Finally, we compose the privacy loss over T communication rounds, incorporate the amplification due to user subsampling, and convert the total RDP to an (ϵ, δ) -DP guarantee.

Step 1: RDP of Local Updates and Transmitted Sketches by Client k w.r.t. \mathcal{D}_k .

Privacy guarantee for first sketching Client k executes LocalUpdateDP (using m local steps, data subsampling ratio s , fixed $A_k^t = A^{t-1}$, and noise parameter σ^2) on its private dataset \mathcal{D}_k to compute the local LoRA matrix B_k^t . By Lemma 5 and Lemma 7, B_k^t satisfies $(\alpha, \mathcal{O}(\frac{mq_D^2(\alpha+1)}{\sigma^2}))$ -RDP w.r.t. \mathcal{D}_k . The first sketch, $Y_k^{\text{proj}} = B_k^t(A_k^t \Omega)$, is derived from B_k^t by post-processing (Lemma 4), since A_k^t and Ω are independent of \mathcal{D}_k in this context. Thus, Y_k^{proj} also satisfies $(\alpha, R_k^{(t)}(\alpha))$ -RDP w.r.t. \mathcal{D}_k , where $R_k^{(t)}(\alpha) = \mathcal{O}(\frac{mq_D^2(\alpha+1)}{\sigma^2})$.

Privacy guarantee for second sketching: After the client k sends Y_k^{proj} to the server, the server computes an orthonormal basis $Q^t = \text{QR}(\sum_{j \in \mathcal{K}_t} Y_j^{\text{proj}})$ and broadcasts Q^t back to the participating clients, including the client k . The client k then computes its second sketch $\tilde{Y}_k^{\text{proj}} = (A_k^t)^T ((B_k^t)^T Q^t)$. The calculation of $\tilde{Y}_k^{\text{proj}}$ utilizes the already privatized matrix B_k^t , the public matrix A_k^t , and the received matrix Q^t . For client k , Q^t is an external input provided by the server, and this computation does not involve fresh access to its private dataset \mathcal{D}_k . Consequently, according to Lemma 6, $\tilde{Y}_k^{\text{proj}}$ also satisfies $(\alpha, R_k^{(t)}(\alpha))$ -RDP with respect to \mathcal{D}_k .

So we could have that, for the local uplink transmitted information, Y_j^{proj} and $\tilde{Y}_k^{\text{proj}}$ satisfy the $(\alpha, R_k^{(t)}(\alpha))$ -RDP w.r.t. \mathcal{D}_k , where

$$R_k^{(t)}(\alpha) = \mathcal{O}(\frac{mq_D^2(\alpha+1)}{\sigma^2}). \quad (20)$$

Step 2: DP guarantee of (A^t, B^t) w.r.t. the Joint Dataset $\mathcal{D} = \bigcup_k \mathcal{D}_k$.

The server aggregates the second sketches to form $\tilde{Y}_{\text{agg}}^t = \sum_{k \in \mathcal{K}_t} \tilde{Y}_k^{\text{proj}}$. Based on the $(\alpha, \epsilon_k^{(t)}(\alpha))$ -RDP guarantee for each client's transmitted information w.r.t. its local data (Step 1) and the disjointness of client datasets, the mechanism producing an appropriately scaled aggregate over the $K_s = |\mathcal{K}_t|$ participating clients yields $(\alpha, R_{\text{agg}}^{(t)}(\alpha))$ -RDP for \tilde{Y}_{agg}^t w.r.t. the joint data $\mathcal{D}_{\mathcal{K}_t} = \bigcup_{k \in \mathcal{K}_t} \mathcal{D}_k$, where

$$R_{\text{agg}}^{(t)}(\alpha) = \epsilon_k^{(t)}(\alpha)/K_s = \mathcal{O}\left(\frac{mq_D^2(\alpha+1)}{K_s \sigma^2}\right). \quad (21)$$

Since the global LoRA matrices (A^t, B^t) are derived via SVD of \tilde{Y}_{agg}^t (a post-processing step, Lemma 4), they inherit this RDP guarantee. Consequently, by applying the RDP to DP conversion (Lemma 6), for any $0 < \delta_0 < 1$, (A^t, B^t) satisfy $(\epsilon_0^{(t)}, \delta_0)$ -DP w.r.t. $\mathcal{D}_{\mathcal{K}_t}$, with $\epsilon_0^{(t)}$ given by:

$$\epsilon_0^{(t)}(\alpha, \delta_0) = R_{\text{agg}}^{(t)}(\alpha) + \ln\left(\frac{\alpha-1}{\alpha}\right) - \frac{\ln \delta_0 + \ln \alpha}{\alpha-1}. \quad (22)$$

Step 3: DP guarantee of (A^T, B^T) w.r.t. the Joint Dataset $\mathcal{D} = \bigcup_k \mathcal{D}_k$.

The per-round guarantee $(\epsilon_0^{(t)}, \delta_0)$ w.r.t. $\mathcal{D}_{\mathcal{K}_t}$ is amplified by client subsampling (ratio q_K from K total clients) using Lemma 3, yielding an $(q_K \epsilon_0^{(t)}(\alpha, \delta_0), q_K \delta_0)$ -DP guarantee per round w.r.t. the full dataset $\mathcal{D} = \bigcup_{i=1}^K \mathcal{D}_i$.

Composing this $(q_K \epsilon_0^{(t)}(\alpha, \delta_0), q_K \delta_0)$ -DP mechanism over T adaptive communication rounds using Lemma 2, for a chosen $\delta_1 > 0$, gives the final (ϵ, δ) -DP guarantee for (A^T, B^T) :

$$\epsilon = q_K \sqrt{2T \ln(1/\delta_1)} \mathcal{O}\left(\frac{mq_D^2(\alpha+1)}{K_s \sigma^2} + \ln\left(\frac{\alpha-1}{\alpha}\right) - \frac{\ln \delta_0 + \ln \alpha}{\alpha-1}\right), \quad (23)$$

$$\delta = q_K T \delta_0 + \delta_1. \quad (24)$$

The specific noise variance σ^2 required in Theorem 1 is derived by appropriately setting $\epsilon_0^{(t)}, \delta_0$ (based on RDP conversion from Step 2) and δ_1 to meet the target overall (ϵ, δ) , then solving for σ^2 .

Step 4: Analysis of the RDP Order α .

Let δ_0 and δ_1 be $\delta/2$ and $\delta/(2q_K T)$ respectively, we now try to acquire an expression of α through the following minimization problem

$$\min_{\alpha > 1} \frac{mq_D^2(\alpha + 1)}{K_s \sigma^2} + \ln\left(\frac{\alpha - 1}{\alpha}\right) - \frac{\ln(\delta/2) + \ln \alpha}{\alpha - 1}. \quad (25)$$

Let $C_1 = \frac{mq_D^2}{K_s \sigma^2}$, equation (25) find an optimal $\alpha > 1$ that minimizes ϵ is approximated by setting the derivative of the dominant terms to zero.

$$C_1(\alpha - 1)^2 + \ln(\delta_0 \alpha) = 0. \quad (26)$$

Assume $\alpha \gg 1$, then, $(\alpha - 1)^2 \approx \alpha^2$ and the term $\ln(\delta_0 \alpha)$ can be written as $\ln \delta_0 + \ln \alpha$.

Substituting these approximations into the condition (26), we get:

$$C_1 \alpha^2 + \ln \delta_0 + \ln \alpha \approx 0. \quad (27)$$

If α is sufficiently large such that $C_1 \alpha^2$ dominates $\ln \alpha$ (i.e., the α^2 term grows much faster than $\ln \alpha$), we can further simplify Eq. (27) by neglecting the $\ln \alpha$ term relative to $C_1 \alpha^2$ and $\ln \delta_0$ (especially if $|\ln \delta_0|$ is large, which is true for small δ_0). This yields:

$$C_1 \alpha^2 \approx -\ln \delta_0. \quad (28)$$

From Eq. (28), we obtain an approximate expression for the optimal α :

$$\alpha_{\text{opt}} \approx \sqrt{\frac{-\ln \delta_0}{C_1}}. \quad (29)$$

Substituting $\delta_0 = \delta/(2q_K T)$ and $C_1 = \frac{mq_D^2}{K_s \sigma^2}$:

$$\alpha_{\text{opt}} \approx \sqrt{\frac{\ln(2q_K T/\delta) \cdot K_s \sigma^2}{mq_D^2}}. \quad (30)$$

Plug (30) into (24), we could conclude that to reach (ϵ, δ) -DP, FedASK necessitates a noise of

$$\sigma^2 = \mathcal{O}\left(\frac{q_D^2 \cdot m \cdot q_K \cdot T \cdot \ln(2/\delta) \cdot \ln(2Tq_K/\delta)}{\epsilon^2 \cdot K}\right). \quad (31)$$

This finishes the proof of theorem 1.

□

A.3 Proof of Theorem 2

Lemma 8 (Expected Frobenius Norm Error of Random Projection [14]). *Let $A \in \mathbb{R}^{m \times n}$ be a matrix with singular values $\sigma_1 \geq \sigma_2 \geq \dots$. Choose a target approximation rank $k_{\text{approx}} \geq 1$ and an oversampling number $s_{\text{over}} \geq 2$ such that the total number of random projection vectors $l = k_{\text{approx}} + s_{\text{over}} \leq \min\{m, n\}$. Let $\Omega \in \mathbb{R}^{n \times l}$ be a standard Gaussian random matrix, and let $Y = A\Omega$. Let P_Y be the orthogonal projector onto $\text{Range}(Y)$. Then, the expected Frobenius norm of the error in approximating A by its projection $P_Y A$ is bounded by,*

$$\mathbb{E} \| (I - P_Y) A \|_F \leq \left(1 + \frac{k_{\text{approx}}}{s_{\text{over}} - 1}\right)^{1/2} \left(\sum_{j > k_{\text{approx}}} \sigma_j^2(A)\right)^{1/2}.$$

Proof. Let the average of local updates be defined as:

$$\Delta \bar{W} = \frac{1}{K} \sum_{k=1}^K B_k A_k. \quad (32)$$

The first sketching follows as:

$$Y^{proj} = \frac{1}{K} \sum_{k=1}^K B_k(A_k \Omega) = \Delta \bar{W} \Omega, \quad (33)$$

where $\Omega \in \mathbb{R}^{n \times (r+p)}$ is standard Gaussian. The dimension of the random subspace is $r + p$.

The second aggregated projection is:

$$\tilde{Y}^{proj} = \frac{1}{K} \sum_{k=1}^K (A_k^\top (B_k^\top Q)) = (\Delta \bar{W})^\top Q \quad (34)$$

Let $\text{SVD}(Q^\top \Delta \bar{W}) = U \Sigma V^\top$.

$$Q^\top \Delta \bar{W} = U \Sigma V^\top \quad (35)$$

The global update $\Delta W^t = B^t A^t = (Q U \Sigma^{1/2})(\Sigma^{1/2} V^\top) = Q U \Sigma V^\top$.

$$\Delta W^t = Q(Q^\top \Delta \bar{W}) = Q Q^\top \Delta \bar{W} \quad (36)$$

The condition $p \geq d_B - r + 2$ implies $r + p \geq d_B + 2$. Since $\text{rank}(\Delta \bar{W}) \leq d_B$, we have $r + p + 2 \geq \text{rank}(\Delta \bar{W})$. Apply Lemma 8 with $A = \Delta \bar{W}$, let the target rank be $k_{\text{approx}} = r + p$, and $s_{\text{over}} = 2$. For $k_{\text{approx}} > \text{rank}(\Delta \bar{W})$, the singular values $\sigma_{k_{\text{approx}}+1}$ and beyond are zero. Therefore, we could come to the conclusion of Theorem 2. \square

B Future Explorations

While FedASK demonstrates notable strengths, we identify the following areas for future exploration:

- **Local Matrix Update Strategies:** FedASK currently fixes the local A_k matrix during differentially private updates in one communication round. Investigating alternating local updates for both A_k and B_k matrices under differential privacy could reveal different learning dynamics and performance trade-offs.
- **Broader Model Applicability:** Our validation of FedASK is currently limited to Large Language Models. Assessing its efficacy and potential adaptations for other architectures, such as vision transformers or diffusion models, remains an open research direction.
- **Advanced Training Paradigms:** The current study focuses on fine-tuning for standard language and reasoning tasks. Extending FedASK to more complex federated and private training paradigms, such as model alignment (e.g., RLHF), presents a valuable avenue for future work.

C More Experiments results

C.1 Error-Bar of Current Experiments

This section presents error bar experiments, reporting the mean \pm standard error of the mean (SEM) over five independent runs, to substantiate the stability and performance of the FedASK framework. These evaluations cover varied differential privacy (DP) budgets and non-IID data distributions for Llama-2-7B and Llama-2-13B models on the dolly-15K and MetaMathQA datasets, respectively. Unless otherwise specified, all other parameters, such as batch size and communication rounds, align with the primary experimental configurations detailed in Section 5.

For these error-bar evaluations, specific learning rates and LoRA ranks were employed. Llama-2-7B experiments (Tables 5 and 7) used LoRA rank $r = 64$. For IID data with varying DP budgets (Table 5), baseline learning rates were 2×10^{-4} (non-DP) and 1×10^{-4} (DP); FedASK and other LoRA methods used 5×10^{-5} (non-DP) and 4×10^{-4} (DP) with gradient clipping of 1.0. For non-IID evaluations at DP $\epsilon = 3$ (Table 7), baseline learning rates were 1×10^{-4} , and LoRA-based methods (including FedASK) used 4×10^{-4} with 1.0 gradient clipping. The Llama-2-13B experiments with IID data (Table 6) utilized a LoRA rank $r = 128$; FedASK learning rates were 5×10^{-4} (non-DP) and 4×10^{-4} (DP), while baselines used 2×10^{-4} .

Table 5: Performance Comparison (Mean \pm SEM from five runs) on Llama-2-7B with Different DP Budgets.

Task	Priv. Budget	FedASK	FedAvg	FFA-LoRA	FedSA-LoRA	FedProx	Scaffold
MMLU	Non-Private	46.34 \pm 0.19	43.13 \pm 2.01	45.72 \pm 0.27	44.63 \pm 0.57	43.55 \pm 1.44	44.49 \pm 1.17
	$\epsilon = 1$	45.79 \pm 0.01	42.82 \pm 0.75	44.15 \pm 1.39	43.16 \pm 0.25	43.00 \pm 1.01	43.53 \pm 0.12
	$\epsilon = 3$	45.88 \pm 0.37	42.43 \pm 0.94	43.82 \pm 1.10	42.30 \pm 1.17	43.07 \pm 0.11	42.88 \pm 0.41
	$\epsilon = 6$	45.73 \pm 0.05	43.46 \pm 0.12	44.02 \pm 1.20	43.30 \pm 0.54	43.00 \pm 0.71	43.43 \pm 0.37
DROP	Non-Private	32.01 \pm 0.08	30.31 \pm 0.11	31.65 \pm 0.31	30.86 \pm 0.37	30.95 \pm 0.04	30.87 \pm 0.86
	$\epsilon = 1$	31.33 \pm 0.10	30.49 \pm 0.94	30.41 \pm 1.31	29.96 \pm 1.08	30.18 \pm 0.67	30.08 \pm 0.42
	$\epsilon = 3$	31.06 \pm 1.02	29.69 \pm 0.43	29.87 \pm 1.47	29.66 \pm 0.26	29.07 \pm 0.57	28.90 \pm 0.15
	$\epsilon = 6$	31.27 \pm 0.10	29.46 \pm 0.15	30.37 \pm 0.97	29.91 \pm 0.65	28.64 \pm 1.07	30.19 \pm 0.01
Human-Eval	Non-Private	14.63 \pm 0.61	13.42 \pm 1.83	14.02 \pm 0.02	12.81 \pm 0.61	12.81 \pm 0.61	14.63 \pm 0.00
	$\epsilon = 1$	13.72 \pm 1.52	11.28 \pm 1.52	12.50 \pm 0.30	11.28 \pm 2.13	8.85 \pm 3.35	8.54 \pm 1.22
	$\epsilon = 3$	14.02 \pm 1.22	7.63 \pm 2.74	11.59 \pm 0.61	8.85 \pm 2.13	10.06 \pm 3.35	9.76 \pm 1.83
	$\epsilon = 6$	15.85 \pm 0.02	9.76 \pm 1.83	11.90 \pm 0.31	10.67 \pm 2.13	8.85 \pm 2.13	9.76 \pm 2.44

Table 6: Performance Comparison (Mean \pm SEM from five runs) on Llama-2-13B with Different DP Budgets.

Task	Priv. Budget	FedASK	FedAvg	FFA-LoRA	FedSA-LoRA	FedProx	Scaffold
GSM8K	Non-Private	51.40 \pm 1.40	46.25 \pm 2.25	48.50 \pm 0.10	50.00 \pm 2.80	47.95 \pm 0.15	46.95 \pm 1.35
	$\epsilon = 1$	24.95 \pm 2.25	16.40 \pm 0.90	14.25 \pm 0.05	14.50 \pm 2.30	16.00 \pm 0.80	16.45 \pm 0.35
	$\epsilon = 3$	25.35 \pm 0.55	19.60 \pm 3.10	18.60 \pm 1.40	21.20 \pm 1.00	20.20 \pm 2.20	18.30 \pm 2.50
	$\epsilon = 6$	24.35 \pm 3.35	20.05 \pm 0.75	19.15 \pm 0.95	18.45 \pm 1.15	22.05 \pm 1.95	20.35 \pm 0.05
GSM8K _{hard}	Non-Private	23.90 \pm 4.80	21.90 \pm 3.90	22.20 \pm 1.00	22.10 \pm 1.30	23.05 \pm 3.05	20.95 \pm 0.85
	$\epsilon = 1$	13.65 \pm 0.65	10.25 \pm 1.45	7.85 \pm 0.15	8.25 \pm 1.65	7.90 \pm 0.70	9.35 \pm 0.25
	$\epsilon = 3$	13.00 \pm 0.40	11.90 \pm 0.80	10.25 \pm 0.25	11.55 \pm 0.25	11.35 \pm 0.55	11.20 \pm 0.20
	$\epsilon = 6$	13.30 \pm 3.60	11.30 \pm 0.80	9.40 \pm 0.20	10.55 \pm 0.35	11.60 \pm 0.70	11.40 \pm 0.60
Math	Non-Private	12.55 \pm 0.75	9.30 \pm 1.00	10.25 \pm 0.55	10.60 \pm 0.10	10.90 \pm 0.80	10.00 \pm 0.20
	$\epsilon = 1$	7.25 \pm 0.35	5.55 \pm 0.35	5.50 \pm 0.30	5.85 \pm 0.25	5.85 \pm 0.25	5.55 \pm 0.25
	$\epsilon = 3$	7.20 \pm 0.60	6.50 \pm 0.40	6.20 \pm 0.20	6.15 \pm 0.25	6.30 \pm 0.10	5.95 \pm 0.45
	$\epsilon = 6$	6.50 \pm 1.10	6.35 \pm 0.15	6.15 \pm 0.15	6.05 \pm 0.15	6.50 \pm 0.20	7.00 \pm 0.10

The inclusion of mean \pm SEM from five runs in these experiments offers robust statistical validation of the delineated advantages of FedASK, reinforcing the conclusions drawn from single-run experiments in the main paper. As detailed in Table 5 and Table 6, FedASK outperforms or performs comparable to baseline methods in non-private settings and DP budgets of $\epsilon \in \{1, 3, 6\}$, frequently producing comparable or reduced SEMs, highlighting its capacity to achieve an effective equilibrium between model utility and privacy preservation. This demonstrated robustness is further evident in scenarios characterized by data heterogeneity; Table 7 reveals FedASK’s consistent maintenance of leading average performance alongside constrained variability, as indicated by the SEMs, across diverse

non-IID Dirichlet distributions ($\alpha \in \{0.1, 0.5, 1.0\}$), corroborating the adaptability observations presented in Section 5.2.

Table 7: Performance Comparison (Mean \pm SEM from five runs) for DP Budget $\epsilon = 3$ across Different Data Distributions on Llama-2-7B.

Task	Data Dist.	FedASK	FedAvg	FFA-LoRA	FedSA-LoRA	FedProx	Scaffold
MMLU	IID	45.88 \pm 0.37	42.43 \pm 0.94	43.82 \pm 1.10	42.30 \pm 1.17	43.07 \pm 0.11	42.88 \pm 0.41
	Dir(0.1)	45.21 \pm 0.84	42.85 \pm 0.16	43.64 \pm 1.09	44.11 \pm 0.16	42.99 \pm 0.39	42.33 \pm 0.73
	Dir(0.5)	45.05 \pm 0.90	42.71 \pm 0.60	43.22 \pm 1.76	43.26 \pm 0.54	42.66 \pm 0.32	42.91 \pm 0.94
	Dir(1)	45.26 \pm 0.75	42.75 \pm 0.21	44.60 \pm 1.37	42.37 \pm 1.33	43.10 \pm 0.12	42.69 \pm 0.98
DROP	IID	31.10 \pm 1.04	29.78 \pm 0.34	29.87 \pm 1.47	29.66 \pm 0.26	29.07 \pm 0.57	28.90 \pm 0.15
	Dir(0.1)	30.85 \pm 0.17	29.27 \pm 0.93	30.52 \pm 0.42	28.72 \pm 0.14	28.53 \pm 0.35	28.29 \pm 0.02
	Dir(0.5)	31.15 \pm 0.01	29.41 \pm 0.23	29.98 \pm 0.72	28.47 \pm 0.64	28.47 \pm 0.24	29.17 \pm 0.28
	Dir(1)	31.19 \pm 0.40	29.77 \pm 0.25	30.16 \pm 1.23	29.40 \pm 0.11	29.85 \pm 0.03	30.20 \pm 0.32
Human-Eval	IID	14.02 \pm 1.22	7.63 \pm 2.74	11.59 \pm 0.61	8.85 \pm 2.13	10.06 \pm 3.35	9.76 \pm 1.83
	Dir(0.1)	13.41 \pm 0.00	9.15 \pm 1.83	11.29 \pm 0.31	10.67 \pm 2.13	9.15 \pm 4.27	8.24 \pm 0.31
	Dir(0.5)	12.81 \pm 1.82	9.76 \pm 1.22	11.89 \pm 1.52	12.19 \pm 0.61	14.33 \pm 0.31	8.24 \pm 1.52
	Dir(1)	13.41 \pm 0.61	7.93 \pm 1.83	12.50 \pm 1.52	10.37 \pm 0.00	7.93 \pm 2.44	7.63 \pm 1.52

C.2 Algorithms within more DP and Non-iid Conditions

Table 8 provides a comparative evaluation of algorithm performance when subjected to the combined effects of differential privacy and specific non-IID data distributions, namely Dirichlet distributions with $\alpha = 0.1$ representing higher data heterogeneity and $\alpha = 1.0$ indicating lower heterogeneity. This side-by-side presentation for each algorithm across various DP budgets ($\epsilon \in \{1, 3, 6\}$ and Non-Private) allows for a nuanced understanding of their robustness.

The results in Table 8 underscore FedASK’s consistent ability to deliver strong performance even under these challenging compound conditions. Across the evaluated tasks (MMLU, BBH, DROP, Human-Eval), FedASK generally maintains a competitive edge or outperforms baseline methodologies for both the more heterogeneous non-IID setting $\alpha = 0.1$ and the less heterogeneous setting $\alpha = 1.0$. In particular, while increased DP noise (smaller ϵ) or increased data heterogeneity (smaller α) tends to degrade performance for all algorithms, FedASK often exhibits a more graceful degradation compared to several baselines. This suggests that FedASK’s two-stage sketching and aggregation mechanism not only preserves utility under DP but also offers resilience against varying degrees of data heterogeneity. The comparative performance between the Non-IID 0.1 and Non-IID 1.0 columns for FedASK within each DP budget further illustrates its capacity to adapt effectively, reinforcing its suitability for practical federated learning scenarios where both privacy and non-IID data are prevalent concerns.

Table 8: Algorithm Performance across Varying DP Budgets for Non-IID (Dirichlet 0.1 and 1.0) Data on Llama-2-7B

Task	DP Setting	FedASK		FedAvg		FFA-LoRA		FedSA-LoRA		FedProx		Scaffold	
		α 0.1	α 1.0	α 0.1	α 1.0	α 0.1	α 1.0	α 0.1	α 1.0	α 0.1	α 1.0	α 0.1	α 1.0
MMLU	No DP	46.50	46.32	45.59	45.61	45.33	45.82	45.82	45.48	45.53	45.51	43.75	44.70
	DP $\epsilon = 1$	45.73	45.88	42.69	42.12	41.00	43.75	41.44	41.62	41.40	43.66	43.11	43.60
	DP $\epsilon = 3$	46.04	45.86	42.69	42.96	42.54	43.23	44.27	41.04	42.61	42.98	43.05	41.71
	DP $\epsilon = 6$	46.24	46.42	41.79	43.97	42.82	42.24	42.94	43.93	40.07	43.56	41.06	43.83
BBH	No DP	32.15	32.55	33.50	32.03	32.16	32.86	32.25	32.11	33.10	32.29	32.99	33.08
	DP $\epsilon = 1$	31.99	31.78	31.14	31.73	31.71	33.45	33.34	31.80	32.22	33.40	32.28	31.36
	DP $\epsilon = 3$	32.46	32.39	33.54	31.02	32.71	32.06	33.37	32.61	32.30	32.17	33.02	31.50
	DP $\epsilon = 6$	32.12	31.91	31.98	30.99	32.42	31.56	31.00	31.65	31.67	34.01	31.12	32.44
DROP	No DP	33.16	32.30	30.56	31.47	31.19	33.46	30.96	31.92	31.09	32.78	28.94	30.12
	DP $\epsilon = 1$	31.93	31.98	28.18	29.93	29.75	31.17	28.96	28.81	28.16	30.71	29.45	29.20
	DP $\epsilon = 3$	31.01	31.09	31.49	30.02	30.10	28.93	28.58	29.29	28.18	29.82	28.27	30.52
	DP $\epsilon = 6$	32.46	30.90	28.78	28.35	29.51	29.21	30.37	26.51	29.96	28.51	28.88	29.80
Human-Eval	No DP	15.24	15.85	12.20	12.80	14.63	14.02	14.02	14.02	12.80	14.02	12.80	15.85
	DP $\epsilon = 1$	14.02	12.20	11.59	10.98	9.76	12.20	10.98	10.98	12.20	12.80	14.02	12.80
	DP $\epsilon = 3$	12.20	13.41	12.20	9.76	10.98	10.98	12.80	10.37	13.41	10.37	7.93	9.15
	DP $\epsilon = 6$	12.20	13.41	6.71	13.41	10.37	10.37	6.71	10.98	11.59	12.80	14.63	12.80

C.3 Sensitive Experiments

C.3.1 Choice on the lora rank

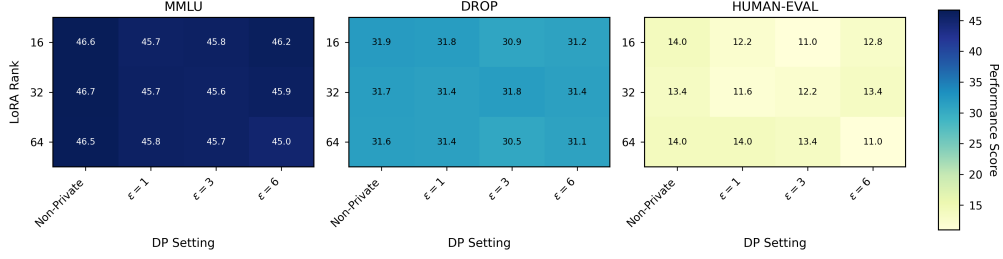


Figure 4: Performance of Llama 2-7B on IID data across LoRA ranks and differential privacy (DP) settings (ϵ) for MMLU, DROP, and Human tasks.

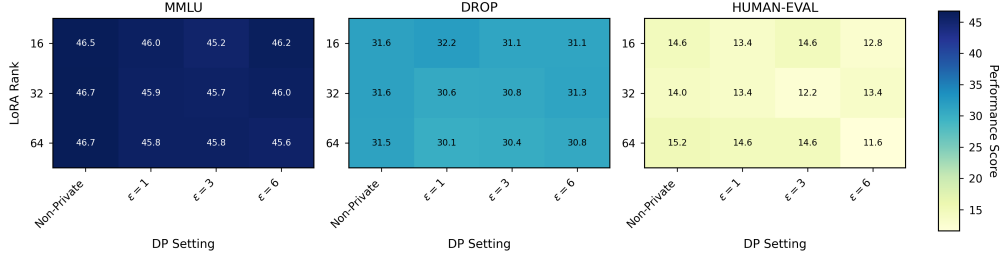


Figure 5: Performance of Llama 2-7B on Non-IID data ($\alpha = 0.1$) across LoRA ranks and differential privacy (DP) settings (ϵ) for MMLU, DROP, and Human tasks.

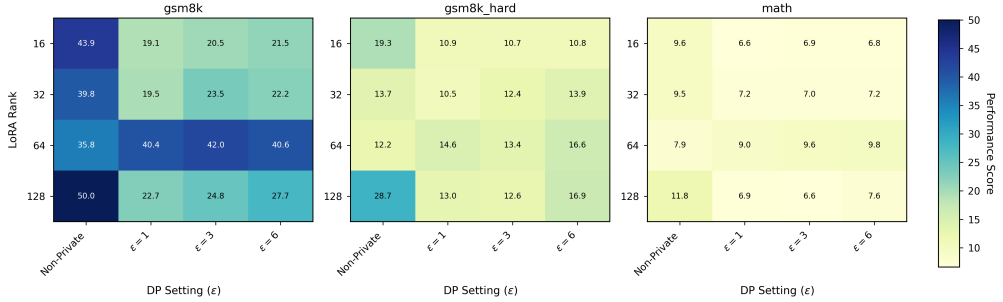


Figure 6: Performance of Llama 2-13B on IID data across LoRA ranks and differential privacy (DP) settings (ϵ) for gsm8k, gsm8k_hard, and math tasks.

The selection of an appropriate LoRA rank r is crucial to balance the performance of the model and the efficiency of the parameters, particularly when differential privacy (DP) is applied. This section details the interaction between LoRA rank, DP settings, model size, and data distribution for the FedASK framework, referencing empirical results from Llama 2-7B and Llama-2-13B models. Although higher LoRA ranks, such as $r = 128$, often deliver superior performance in nonprivate scenarios, the introduction of DP mechanisms significantly alters these performance landscapes, often favoring intermediate ranks for a more robust utility-privacy trade-off.

A key finding, illustrated in Figure 6 for the Llama 2-13B model on IID data, is the change in the optimal LoRA rank under DP for FedASK. Although rank 128 excels without privacy, for instance, on gsm8k (50.0) and gsm8k_hard (28.7), intermediate ranks frequently provide a superior utility-privacy trade-off when DP is enabled. Specifically, on the gsm8k task, rank 64 consistently outperforms rank

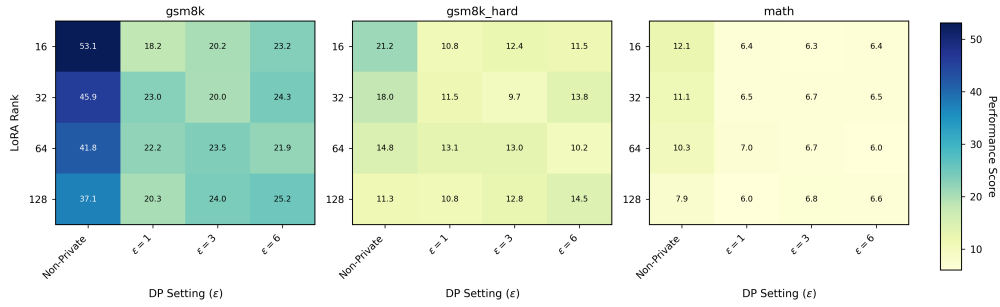


Figure 7: Performance of Llama 2-13B on Non-IID data ($\alpha = 0.1$) across LoRA ranks and differential privacy (DP) settings (ϵ) for gsm8k, gsm8k_hard, and math tasks.

128 under all tested DP settings; for example, with $\epsilon = 1$, rank 64 achieves 40.4 versus 22.7 for rank 128, and with $\epsilon = 6$, rank 64 achieves 40.6 versus 27.7 for rank 128. Similarly, for the math task, rank 64 shows better performance than rank 128 across all DP budgets. On gsm8k_hard, rank 64 also remains highly competitive with, or slightly better than, rank 128 under DP conditions. This consistent strong performance of rank 64 under various DP constraints suggests that for FedASK with the 13B model on IID data, a moderately sized LoRA rank can be more parameter-efficient and achieve better utility when stringent privacy guarantees are necessary. When data heterogeneity is introduced for the Llama 2-13B model, as shown in Figure 7 for Non-IID data ($\alpha = 0.1$), the utility of intermediate ranks under DP persists largely. Although overall performance levels may adjust due to the non-IID distribution, FedASK with moderately sized ranks continues to demonstrate a strong balance between adaptation capability and resilience to DP noise, reinforcing the notion that maximal ranks are not universally optimal under privacy constraints in heterogeneous settings.

This rank-dependent performance pattern under DP is also investigated for the Llama 2-7B model. Figure 4 presents results on IID data for MMLU, DROP, and HumanEval tasks. For FedASK, it is generally observed that while larger ranks might offer marginal gains or lead in non-private scenarios, the application of DP tends to make intermediate ranks more advantageous. These moderately sized ranks appear to strike an effective balance, providing sufficient capacity for task adaptation while mitigating the detrimental impact of DP noise that can be more pronounced with a larger number of trainable parameters. The introduction of significant data heterogeneity with Non-IID data ($\alpha = 0.1$), illustrated in Figure 5, further tests this dynamic. Even in these challenging conditions, FedASK with intermediate ranks often maintains robust performance relative to larger ranks under DP. This suggests that for the 7B model, an excessively large rank under combined DP and non-IID stress may not yield proportional benefits and could be outperformed by more parameter-efficient intermediate rank configurations.

C.3.2 Choice on over-sketching rate

The precision of FedASK’s aggregation mechanism is theoretically linked to the choice of the over-sketching parameter p , which, together with the LoRA rank r , defines the sketching dimension $r + p$. While Theorem 2 provides a condition for exact aggregation, it is crucial to empirically assess the impact of varying sketching dimensions on aggregation fidelity under practical conditions, including different degrees of data heterogeneity and client participation numbers. This appendix section details these specific evaluations for FedASK, illustrating its robustness. The experiments summarized here were conducted to determine a suitable range for the sketching dimension, ensuring high fidelity without unnecessary computational overhead. All results presented pertain to the FedASK algorithm, and aggregation fidelity is quantified as the cosine similarity between the global LoRA update reconstructed by FedASK and the ideal average of true local LoRA updates.

The empirical investigation involved evaluating the aggregation fidelity of FedASK across a matrix of conditions, as depicted in Figure 9. The experiments systematically varied: (i) the sketching dimension (x-axis values: 6, 32, 51, 64, and 96), (ii) the degree of non-iid degree (Dirichlet distributions with $\alpha \in \{1.0, 0.8, 0.5, 0.1\}$), and (iii) the number of participating clients, shown in four distinct panels: (a) 5 clients, (b) 10 clients, (c) 15 clients, and (d) 20 clients. For these specific

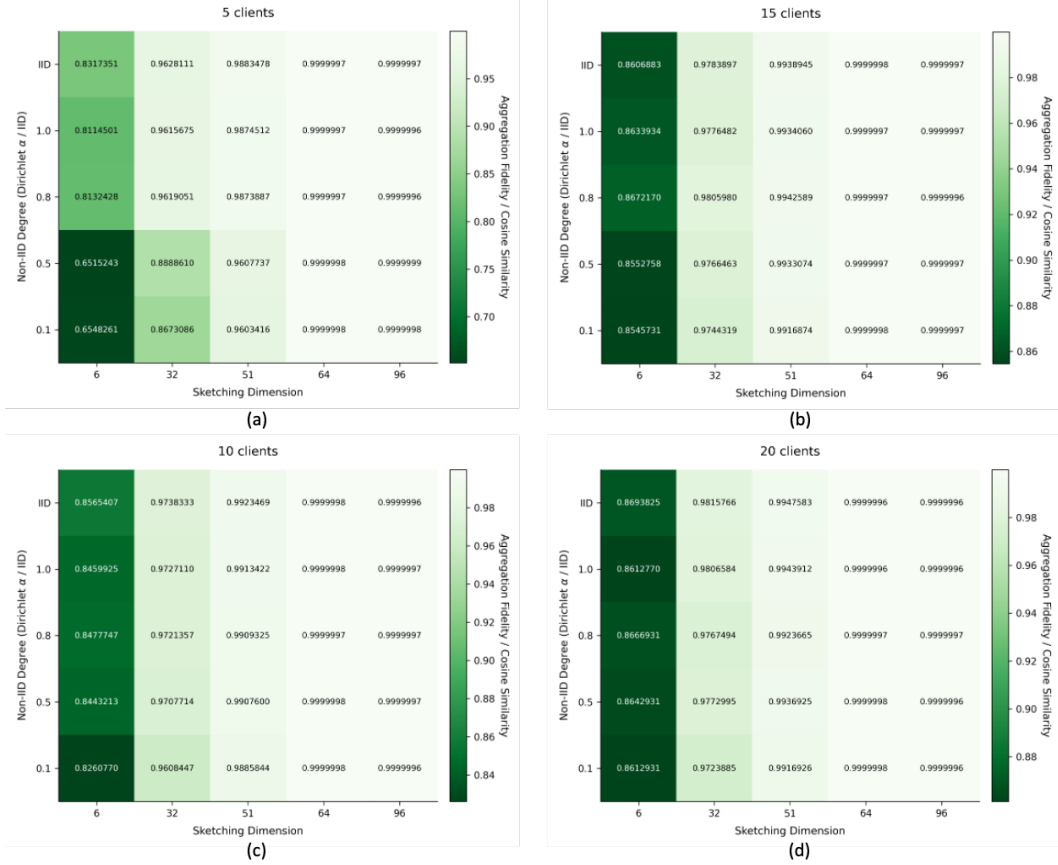


Figure 8: Impact of sketching dimension (x-axis) and non-IID degree (y-axis, Dirichlet α / IID) on FedASK’s aggregation fidelity (cosine similarity) for (a) 5, (b) 10, (c) 15, and (d) 20 clients, showing robust near-unity performance.

fidelity evaluations, differential privacy mechanisms were not applied to isolate the performance of the aggregation mechanism itself. The color intensity in each heatmap cell corresponds to the achieved cosine similarity, with lighter shades indicating higher fidelity.

The results consistently demonstrate FedASK’s exceptional aggregation fidelity across the vast majority of tested scenarios. As seen in Figure 8, near-unity cosine similarity is achieved for most combinations of sketching dimensions, non-IID degrees, and client numbers. Even with the smallest sketching dimensions, fidelity remains remarkably high, particularly as the number of participating clients increases (panels b, c, and d). While the 5-client scenario (panel a) shows slightly reduced fidelity under extreme non-IID conditions and very small sketching dimensions, the performance rapidly approaches unity with modest increases in either parameter. These findings underscore that FedASK is not highly sensitive to the over-sketching rate for maintaining precise aggregation and can achieve excellent fidelity even with minimal or conservative sketching dimensions, confirming its practical efficiency and robustness.

C.4 System Efficiency Experiments

To assess the system efficiency of the federated learning algorithms evaluated, we measured key resource utilization metrics for a single client operating within a federated network of 5 clients. These experiments were carried out on NVIDIA H100 GPUs. The primary metrics, communication volume and peak GPU memory consumption, are detailed for Llama 2-7B and Llama 2-13B models trained with 4-bit precision.

Figure 9 illustrates the usage of resources per client. The volume of communication, segmented into uplink and downlink traffic, is reported in millions of parameters. Peak

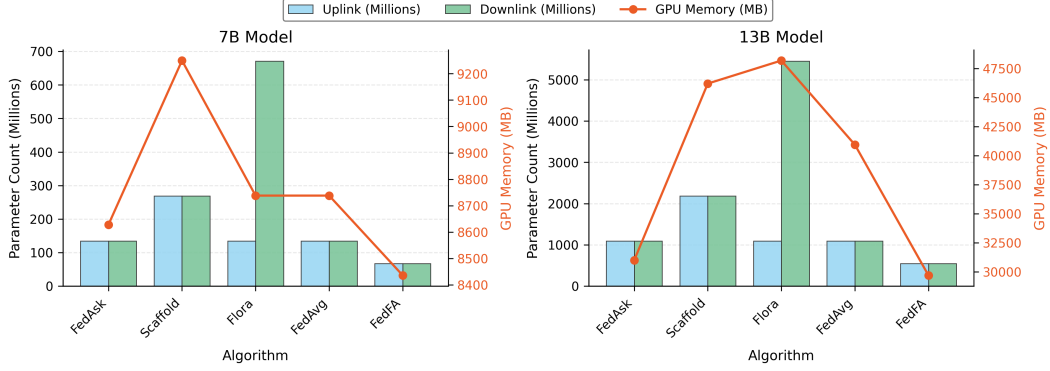


Figure 9: System resource utilization for five federated learning algorithms when training Llama 2-7B (left) and Llama 2-13B (right) models using 4-bit precision. The metrics, shown for a single client in a 5-client federated setup, include uplink and downlink communication volume (millions of parameters) and GPU memory consumption (MB).

Table 9: Total communication volume per client round for federated learning algorithms using Llama 2-7B and Llama 2-13B models under different numerical precisions. All values are in Megabytes (MB).

Algorithm	Llama 2-7B (MB)			Llama 2-13B (MB)		
	FP16	INT8	INT4	FP16	INT8	INT4
FedAsk	512	256	128	4160	2080	1040
Scaffold	1024	512	256	8320	4160	2080
Flora	1536	768	384	12 480	6240	3120
FedAvg	512	256	128	4160	2080	1040
FedFA	256	128	64	2080	1040	520

GPU memory consumption (in MB) was meticulously monitored on the client side using the `torch.cuda.max_memory_allocated(device=torch.device('cuda'))` PyTorch function, capturing the maximum memory footprint during local training operations with differential privacy mechanisms enabled. Furthermore, Table 9 quantifies the total communication volume (uplink plus downlink, in MB) per client round with different numerical precisions (FP16, INT8, and INT4) for both models Llama 2 sizes. This provides a comparative view of how the precision of the data impacts the communication overhead for each algorithm.

System efficiency evaluations highlight distinct resource profiles. FedFA achieves the lowest communication parameter counts by freezing its A matrix, as shown in Figure 9. FedASK, engineered to update both LoRA adapters for enhanced learnability, offers substantial communication efficiency; its INT4 communication volume detailed in Table 9 is approximately 50% less than Scaffold and roughly 66.7% less than Flora. Regarding GPU memory, Figure 9 indicates FedASK’s footprint is comparable to FedAvg and Scaffold but notably less than Flora—for instance, around 23.9% less for the Llama 2-13B model.